Journal of Materials Chemistry B

ROYAL SOCIETY OF CHEMISTRY

REVIEW

View Article Online
View Journal | View Issue

Cite this: J. Mater. Chem. B, 2022, 10, 843

Carbon dot composites for bioapplications: a review

Jiajia Wu,[a] Gonglin Chen,[a] Yinnong Jia,[b] Chunyu Ji,[a] Yuting Wang,[b] Yiqun Zhou,[c] Roger M. Leblanc[c] and Zhili Peng *[a]

Received 9th November 2021,
Accepted 24th December 2021

DOI: 10.1039/d1tb02446a

rsc.li/materials-b

Carbon dots (CDs) have received extensive attention in the last decade for their excellent optical, chemical and biological properties. In recent years, CD composites have also received significant attention due to their ability to improve the intrinsic properties and expand the application scope of CDs. In this article, the synthesis processes of four types of CD composites (metal–CD, nonmetallic inorganics–CD, and organics–CD as well as multi-components—CD composites) are systematically summarized first. Then the recent advancements in the bioapplications (bioimaging, drug delivery and biosensing) of these composites are also highlighted and discussed. Last, the current challenges and future trends of CD composites in biomedical fields are discussed.

1. Introduction

Carbon dots (CDs) are a group of quasi-spherical nanoparticles with sizes smaller than 10 nm,[1] which were first discovered accidentally in 2004 by researchers from the United States during the separation and purification of single-walled carbon nanotubes (SWCNTs) by gel electrophoresis.[2] CDs did not receive much attention until a groundbreaking report from Sun's group in 2006.[3] Structurally speaking, CDs are generally considered to possess carbonized cores (either crystalline or amorphous) with functionalized surfaces which could contain various functionalities such as carbonyls, carboxylic acids, hydroxyls, epoxides, amines, *etc.*[4–6] The nature and properties of CDs' surfaces are easily influenced by the precursors used and synthesis methods adopted during the synthesis of CDs,[7,8] thus rendering CDs with the advantage of facile surface modifications. Syntheses of CDs are simple and versatile, which could be classified into two approaches, namely "top-down" and "bottom-up".[9] The "top-down" method generally involves the cleavage of large carbonaceous materials into small CDs *via* harsh treatments such as arc discharge, laser ablation,[10,11] and electrochemical stripping[12] as well as acidic oxidation treatment.[13,14] The "bottom-up" approach involves the polymerization and carbonization of small carbon-containing molecules into CDs,[15] which could be realized through microwave[16] or hydrothermal/solvothermal treatments.[17]

In the past decade, the field of CDs has advanced significantly, as evidenced by their wide applications in various fields such as chemistry, physics, engineering and optoelectronics.[18–20] Among them, CDs are especially known for their cross applications in biomedical fields considering their unique photoluminescence (PL) properties, excellent photostability, extraordinary biocompatibility, tunable surface functionalities, facile syntheses, as well as economic accessibility.[21–25] As a result, CDs have been widely investigated for their potential applications in bioimaging, biosensing as well as drug and gene delivery[26–31] in the last decade (Fig. 1). In light of the emerging studies on the biomedical applications of CDs, various excellent review articles have been published on this topic.[32–36] For instance, recent advancements of near-infrared (NIR) C-dots and their biomedical applications have been systematically summarized by Xiong's[37] and Qu's groups.[38] Reviews focused on one specific application of C-dots in biosensing,[39,40] phototherapy,[41] and nanomedicine[42,43] as well as bone tissue engineering[44] have also been published. Even though significant progress has been achieved, applications of CDs in biomedical fields still face some challenges. For instance, although enormous efforts have been devoted, majority of (NIR) CDs still suffer from relatively low PL quantum yields (QYs), significantly limiting their practical applications for bioimaging and theranostics development. Furthermore, the detection process of CDs in biosensing is often interfered with by potential interferents due to the absence of specific recognition groups on the surface of CDs for analytes. Most importantly, the interactions of CDs with biological systems are generally poor and lack specificity,[45] significantly limiting their potential clinical applications.

[a] School of Materials and Energy, Yunnan University, Kunming 650091, People's Republic of China. E-mail: zhilip@ynu.edu.cn; Tel: +86–871–65037399
[b] Yunnan Provincial Key Laboratory of Pharmacology for Natural Products, School of Pharmaceutical Sciences, Kunming Medical University, Kunming 650500, People's Republic of China
[c] Department of Chemistry, University of Miami, 1301 Memorial Drive, Coral Gables, Florida 33146, USA

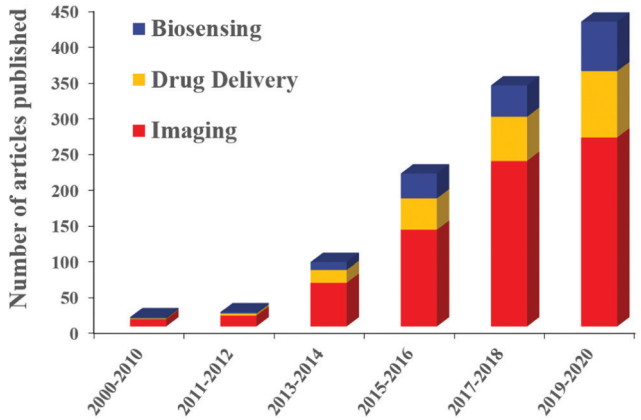

Fig. 1 Number of articles published on the applications of CDs in biomedical fields, results obtained *via* Google Scholar on September 6th, 2021. Blue, yellow and red columns represent articles resulting from searching by the exact phrases "carbon dots, carbon nano dots, carbon quantum dots, graphene quantum dots and C-dots" with "biosensing", "drug delivery", and "imaging" occurring in the title of a paper, respectively.

CD composites have turned out to be very successful in addressing the above-mentioned issues, and surface functionalization and heteroatom doping have proven to be among the most effective methods to obtain them.[46,47] Up to now, various traditional materials such as metals/metal oxides, nonmetallic inorganic materials as well as organics have been widely composited with CDs to enhance their intrinsic properties and expand their application scope. In these systems, the merits are obvious by compositing CDs with traditional materials regarding their bioapplications. Firstly, the PLQYs of CDs could be generally increased by either compositing with metals and small organic molecules or direct element doping; furthermore, by properly tuning the compositing reagents, red-shift of the fluorescence emissions could be achieved for the resulted CD composites compared to that of bare CDs. The enhancements in the PLQYs and red-shift of the fluorescence emissions are extremely important for the further advancement of CDs in biomedical fields. Secondly, CD composites could be endowed with some unique features that are highly advantageous for bioapplications but impossible to see in bare CDs. For instance, by compositing with ferromagnetic materials, CD composites could be applied for dual mode (fluorescence and MRI) imaging, which is impossible to achieve in bare CDs. By compositing with metals or polymers, the mechanical strength of CDs could be greatly enhanced, which are rather important for their applications as scaffolds for bone tissue engineering. Thirdly, the composition of CDs with other molecules such as antibodies and nucleic acids could significantly enhance their sensitivity and specificity towards analytes, greatly expanding their application scope in biosensing. Lastly, the interactions of CDs with biological systems generally lack specificity, which limit their potential clinical applications. By compositing with proper molecular ligands, this shortcoming could be much alleviated. For instance, many reports have demonstrated that CDs could obtain high cancer targeting ability by functionalizing with appropriate ligands. Indeed, studies have undoubtedly demonstrated the effectiveness of composites in improving the properties of CDs, enhancing their performances in various applications and expanding their application scope.[48,49]

Despite the advancements, reviews specifically focus on CD composites and their biomedical applications have been relatively limited in the literature. Currently, there are some summaries related to CD composites; however, these reviews are generally sporadic and limited to a specific type of materials composited with CDs.[50–52] Thus, a comprehensive review that specifically focuses on CD composites and summarizes their biomedical applications systematically is still missing. In this context, this review aims to summarize the recent advancements in the synthesis of CD composites and their applications in biomedical fields. Firstly, we will discuss various materials that are composited with CDs, with an emphasis on their synthesis approaches. In this section, four types of CD composites, namely metal–CD, nonmetallic inorganics–CD, organics–CD, as well as multi-components–CD composites, will be discussed in detail (Fig. 2). Secondly, we will carefully discuss the biomedical applications of these CD composites, including bioimaging, drug delivery and biosensing. Lastly, perspectives on the challenges and future trends of CD composites will be provided.

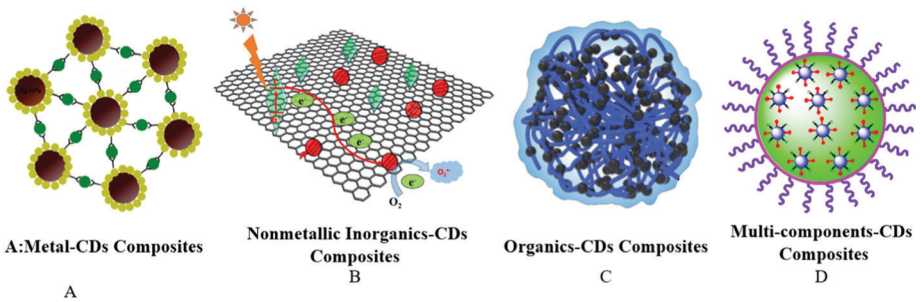

Fig. 2 Cartoon representation of (A) metal–CD composites. Reproduced with permission from ref. 53. Copyright 2017, Elsevier. (B) Nonmetallic inorganics–CD composites. Reproduced with permission from ref. 54. Copyright 2016, Elsevier. (C) Organics–CD composites. Reproduced with permission from ref. 55. Copyright 2019, WILEY-VCH. (D) Multi-components–CD composites. Reproduced with permission from ref. 56. Copyright 2016, American Chemical Society.

2. Synthesis of CD composites

There are mainly three types of materials compounded with CDs, namely metals, nonmetallic inorganics and organics. Interestingly, syntheses of these CD composites are very similar and could be realized *via* physical mixing (*i.e.*, stirring and ultrasonication), and hydrothermal/solvothermal treatment, as well as microwave assisted treatment. Depending on the actual experiments undertaken, these methods can be regarded as either a one-pot or stepwise approach. One-pot synthesis refers to reactions in which all the precursors are treated together, so that the syntheses of CDs as well as their composites with other materials are carried out all at once. This approach is relatively simple, cheap and efficient; however, it generally suffers from inefficient control over the desired properties (*i.e.*, size, surface chemistry, *etc.*) of the composites formed. On the other hand, in the stepwise approach, CDs are prepared in advance, and follow-up reactions are generally required to compound them with other selected materials. This approach generally displays a wider selection of components and behaves better in tuning the properties of the composites compared to the one-pot approach.

2.1. Synthesis of metal–CD composites

Metal–CD composites are a major type of CD-based composites and formed by composition of CDs with metals/metal oxides. Metals, including noble metals and transition metals, have been widely applied in optoelectronic, biomedicine and other fields because of their unique electrical and optical properties.[57,58] As a result, compositing metals with CDs to improve the photoelectric properties of CDs has attracted great attention.[59–61] Depending on the structure of the composites formed, there are mainly three forms of metal presented in the metal–CD composites, including metal ions/atoms, metal nanoparticles (MNPs) and metal oxides (MOs).[62–65]

For the first type, it is generally regarded as metal ion/atom doping, which not only improves the optical properties of CDs but also gives novel functionalities to CDs because of the modulation in the band structure. In most studies, composites of metal ions/atoms and CDs are mainly presented in the form of M@CDs and can be obtained through hydrothermal and chemical reduction[66,67] (Fig. 3A). Strictly speaking, this type of composite is generally considered as metal-doped CDs, not CD "composites". On the other hand, MNPs are the most common form in metal–CD composites and can be prepared *via* both physical (*i.e.*, simple mixing and stirring) and chemical (*i.e.*, reduction) means. In the physical method, MNPs are generally prepared in advance, and they are normally formed through the reduction of metal ions *in situ* through chemical methods.[68] MNPs and CDs are mainly compounded in the form of MNPs@CDs (Fig. 3B); however, sometimes they also form structures of CDs@MNPs (Fig. 3C) type through covalent bonding.[69–71] In addition, some of them can also form a core–shell structure (Fig. 3D), in which MNPs function as the core, and CDs cover the surface to form the shell.[72] Lastly, MOs are also commonly recognized as important components in the metal–CD composites and they generally form very uniform structures with CDs due to their excellent interactions with CDs[73] (Fig. 3E). MO–CD composites are mainly prepared through hydrothermal/solvothermal treatment.[74,75] As can be seen, due to the presence of different forms of metals in the composites, as well as their different application purposes, synthesis methods for the preparation of metal–CD composites are also quite diverse. Among various methods, physical mixing, hydrothermal/solvothermal treatment and chemical reduction are the most frequently adopted approaches.

2. 1.1. Synthesis *via* physical mixing. In this method, metal–CD composites are prepared by mixing CD solution with metal salt solution (or dispersion of MNPs), and the interactions of metals with CDs are generally facilitated by mechanical shearing, stirring and mixing, ultrasonic treatment as well as mild heating. This synthesis approach generally experiences very mild reaction conditions and is environment-friendly. However, the interactions of metals and CDs in the composites are normally poor.[76] For instance, in a recent study, CDs were first synthesized *via* solvothermal treatment, then the as-prepared CDs were stirred with alkali metal solutions to generate the desired M@CDs composites.[77] Interestingly, these metal-ion-functionalized CDs demonstrated excellent red-emissive PL properties with QYs of 34.09% (Li@CDs), 29.29% (Na@ CDs) and 27.64% (K@CDs). The higher QY demonstrated by Li@CDs was attributed to the fact that Li atoms exhibit higher electronegativity than Na and K. Unfortunately, the authors did not compare these composites with their counterparts, the metal-free

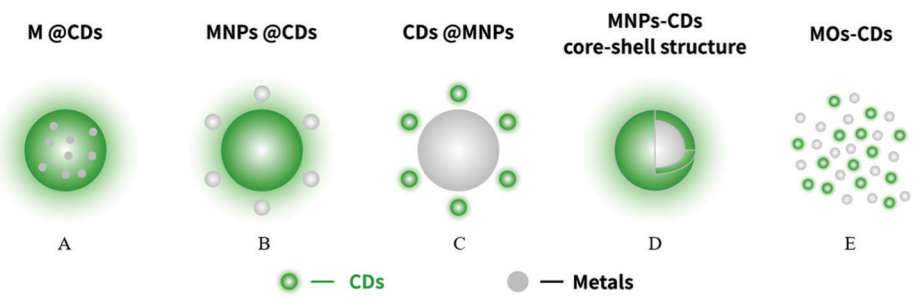

Fig. 3 Cartoon representation of the possible structures of metal–CD composites: (A) M@CDs, metal ions in the CDs; (B) MNPs@CDs, metal nanoparticles on the surface of CDs; (C) CDs@MNPs, CDs on the surface of metal nanoparticles; (D) MNP–CD core–shell structure, metal nanoparticles as the core and CDs as the shell; and (E) MO–CD, metal oxides and CDs form uniform structures.

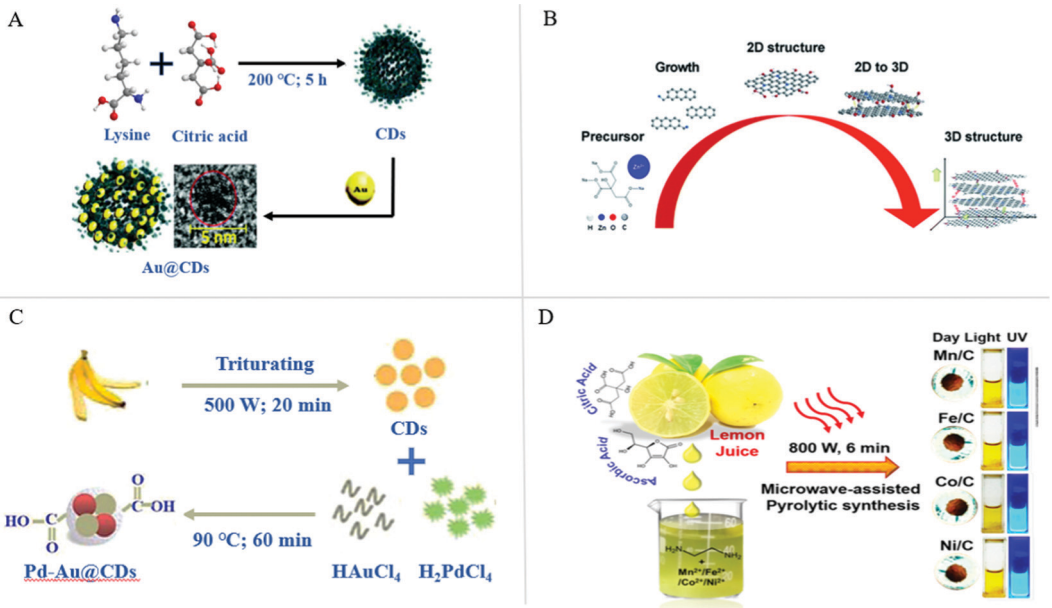

Fig. 4 (A) Schematic illustration of the synthesis process of Au@CDs. Reproduced with permission from ref. 78. Copyright 2020, The Royal Society of Chemistry. (B) Schematic diagram showing the growth of Zn–CDs from an sp^2 to an sp^3 structure. Reproduced with permission from ref. 80. Copyright 2018, The Royal Society of Chemistry. (C) Schematic illustration of the synthesis process of Pd/Au-CDs. Reproduced with permission from ref. 61. Copyright 2017, Elsevier. (D) Schematic illustration of the synthesis process of metal ion (Mn^{2+}, Fe^{2+}, Co^{2+}, Ni^{2+})-doped CDs. Reproduced with permission from ref. 63. Copyright 2018, American Chemical Society.

CDs. Applying similar strategies, CDs were also composited with various MNPs (*i.e.*, Au, Ag, and Pt) (Fig. 4A).[78] In addition to metal atoms/ions and MNPs, the composites of CDs with MOs have also been achieved through physical mixing.[79] As demonstrated, physical mixing is a facile method to prepare metal–CD composites. However, it is worth noting that a majority of metal–CD composites are synthesized *via* other methods such as hydrothermal/solvothermal treatment, microwave-assisted method and electrochemical synthesis.

2.1.2. Synthesis *via* hydrothermal/solvothermal treatment. Currently, hydrothermal treatment is the most widely used approach for the preparation of metal–CD composites. It is environment-friendly, easy to operate and has a unified reaction system; however, the reaction time could be long and reaction conditions are generally harsh (*i.e.*, high temperature and pressure). Hydrothermal treatment could be used to obtain composites with controlled size and shape, and establish strong interactions between the MNPs and CDs. Similarly, syntheses of metal–CD composites *via* hydrothermal treatment could be broadly divided into one-pot and stepwise approaches.

In the one-pot approach, the preparation of CDs and their composition with metals are achieved simultaneously in a one-pot fashion by mixing and treating the precursors of CDs and solutions of metal salts altogether. For example, Xu *et al.* synthesized Zn@CDs using this one-pot hydrothermal treatment and the obtained composites demonstrated uniform sizes (3–10 nm) and bright blue fluorescence with QYs > 32%.[81] Interestingly, the same group demonstrated that the QY (35%) could be fine-tuned by manipulating the reaction time without affecting the morphologies of the composites (Fig. 4B).[80] They attributed the increase of the QY of the Zn–CDs to the fact that Zn could directly oxidize carbon-based surface passivation and prevent the aggregation of graphene π–π stacking. With the understanding of the PL mechanism of metal–CD composites, the same group further pushed their work in this area and successfully realized the synthesis of the metal–CD composite (Ba@CDs) with quantitative yield (99.6%). Unlike in the case of Zn–CDs, the authors attributed the high QY to the defected structures on CDs caused by the charge transfer from Ba atoms.[82] In a different study, Cheng and co-workers realized a high QY of 51.2% on the Zn–CD composite, which they attributed to the radiative recombination of electrons and holes trapped on the CD surface.[67] As can be seen, the PL mechanisms of those metal–CD composites with high QYs varied depending on the specific synthesis methods and compositing metals, which included the increase of radiative pathways (*i.e.*, surface states) of high QYs,[67,82] alleviation of fluorescence quenching,[80] *etc.* With a similar strategy, Cu^{2+}@CDs and La@CDs have also been successfully prepared.[83,84] The stepwise approach refers to reactions in which CDs are prepared separately before they are treated hydrothermally with metals to generate the composites. For instance, Yu *et al.* successfully prepared the TiO_2/CD composite *via* hydrothermal treatment (140 °C for 4 h), in which the CDs were synthesized *via* electrochemical treatment in advance.[85]

Depending on the nature of the carbon precursor, as well as the purpose to control the particle size and shape of the composites, solvents other than water could be used. For example, Zhu *et al.* synthesized a CD-decorated $NiCo_2O_4$ nanohybrid by a two-step solvothermal method, in which ethylene

glycol was used.[86] Interestingly, in this stepwise approach, when composited with noble metals (NMs), CDs tend to deposit onto the surfaces of NMs, forming "CDs@MNPs" type structures (Fig. 3C).[87] The composites of CDs with NMs (*i.e.*, Au, Ag, and Pt) are generally mutually beneficial: firstly, during the synthesis of NM/CD nanohybrids, CDs with abundant oxygen-containing functional groups (*i.e.*, carboxyl and hydroxyl groups) could prevent NMs from aggregation and ensure the activity of NMs by engineering the properties (*i.e.*, sizes) of NMs.[88,89] Secondly, the hybridized NMs also facilitate the realization of high dispersibility of CDs. Most notably, the superior electronic properties of both CDs and NMs can facilitate the electron transfer, resulting in the restriction of charge carrier recombination by an ultrafast relaxation process of localized surface plasmon resonance (LSPR) induced hot electrons,[90] which can boost the performance toward more effective environmental sensing, pollutant treatment and energy conversion.[91,92]

2.1.3. Synthesis *via* chemical reduction. Chemical reduction is a conventional method for the syntheses of metal–CD composites, which refers to the preparation of metal–CD composites by reducing metal precursors to MNPs and then compounding with CDs. For instance, Huang *et al.* synthesized Au@CDs by reducing $HAuCl_4$ with sodium citrate, and then mixed with CDs at 100 °C for 80 min.[93] With similar strategy, Liu and co-workers prepared CDs which could be adsorbed on surface of AuNPs through electrostatic interaction.[94] In these syntheses, commonly used reductants for the reduction of metal ions include boron hydride, sodium citrate, *etc.*[93–95] However, these reductants are dangerous chemicals and easily introduce by-products during synthesis, thus methods for the preparation of metal–CD composites without these traditional reductants are greatly desired.

Considering the fact that there are generally rich reducing functionalities (*i.e.*, amines, alkenes, *etc.*) on CDs, it might be possible to use CDs separately and directly to reduce metal ions by accelerating electron transfer and stabilize the formed MNPs. Indeed, studies have demonstrated the possibility of using CDs as reductants in the preparation of MNP–CD composites.[96] Depending on the nature of the CDs used, the reaction conditions for the reduction of metals can vary significantly. For example, to prepare AuNP–CD core–shell nanocomposites, Sonam *et al.* mixed $HAuCl_4$ solution and CDs at room temperature, while Luo and co-workers applied a much harsher condition (100 °C). In these two examples, CDs were synthesized by microwave irradiation and an electrochemical method, respectively.[97,98] Interestingly, the QY of the AuNP–CD composite was only 0.5% in Luo's study, and this extremely low QY was attributed to the quenching effect arising from the photoinduced electron transfer from CD shells to Au cores and the nucleation of CDs.[99] In addition to the composition with single NMs, Huang and co-workers also reported the composition of Pd and Au with CDs, and the composite (Pd–Au@CDs) demonstrated a relatively higher QY of 16% (Fig. 4C).[100] Inspired by these studies, Ag–CD nanocomposites have also been reported.[101]

Generally speaking, noble metal ions tend to accumulate on the surface of CDs owing to the abundance of oxygen-containing groups during chemical reduction; this process could promote the formation of noble MNPs, leading to a reverse core–shell structure (see Fig. 3D, where CDs is the core and MNPs is the shell instead). This technique has the advantage of a short preparation time and simple reaction conditions (*i.e.*, room temperature and atmospheric pressure); however, it could be difficult to control the size of MNPs and it might potentially pollute the environment.

2.1.4. Synthesis *via* other preparation methods. In addition to the above-mentioned methods, some other preparation methods such as microwave-assisted synthesis and the sonochemical method are commonly used. For instance, Sajid *et al.* reported ethylenediamine-functionalized transition metal ion-doped CDs by microwave-assisted pyrolysis at 800 W for 6 min. Compared to the QY of the pristine CDs (48.31%), the synthesized Mn^{2+}@CDs, Fe^{2+}@CDs, Co^{2+}@CDs, and Ni^{2+}@CDs exhibited QYs of 35.71, 41.72, 75.07, and 50.84%, respectively. The authors suggested that the enhancement or quenching of PL depended on the interactions of transition-metal ions that acted as dopants with the surface of CDs. The Co^{2+}@CDs presented the highest QY, which was attributed to the fact that Co^{2+} prevented the formation of complexes and the secondary amine moieties were bound to the primary oxy-functional groups on the

Table 1 Selective examples for the synthesis of metal–CD composites

Composite form	Carbon source[d]	Synthesis method[e]	Reaction parameters	Size (nm)	QY[f] (%)	Application	Ref.
Li@CDs	CA; urea	PM	1/60 h	3–5	34.09	pH sensing	77
Au@CDs	CA; Lys	PM	37 °C, 1/3 h	3.9–4.7	—	Colorimetric sensing	78
Zn@CDs	SC	Hydrothermal	185 °C, 1–10 h	3–10	34.6	Biosensor	80
Cu^{2+}@CDs	Tea	Hydrothermal	150 °C, 6 h	−0.85	3.26	Nanoprobe	83
La@CDs	ATP	Hydrothermal	160 °C, 8 h	3.97–4.64	13.9	Biosensor, bioimaging	84
TiO_2/CDs	Graphite	Hydrothermal	140 °C, 4 h	20–30	—	Photocatalytic	85
CDs-MOs[a]	Graphite	Solvothermal	180 °C, 3 h	250–350	—	Supercapacitor	86
Pd/Au–CDs	BP	CR	90 °C, 1 h	5–15	16	Biosensor	100
M@CDs[b]	CLE	Microwave	800 W, 1/10 h	2.72–3.69	35.71–75.07	Bioimaging	102
M@CDs[c]	PEG	Sonochemical	3 h	6–8	1.8–16	Cell labeling	103
Ag@CDs	GR	PM	1/2 min	∼4	—	Immunosensor	105
CDs@Pt	LasA	PM	48 h	∼10	—	Biosensor	106

[a] MOs = $NiCo_2O_4$. [b] M = Mn, Fe, Co and Ni. [c] M = Ga, Sn, Zn, Ag and Au. [d] CA: citric acid; Lys: L-lysine; GR: graphite rod; LasA: L-ascorbic acid; SC: sodium citrate; ATP: adenosine disodium triphosphate; BP: banana peel; CLE: citrus lemon extract; PEG: polyethylene glycol. [e] PM: physical mixing; CR: chemical reduction. [f] QY: quantum yield.

surface emissive trap sites of CDs (Fig. 4D).[102] In a different study, Vijay *et al.* reported a one-step sonochemical synthesis of a series of CDs from PEG with five different metals (Ag, Au, Ga, Sn and Zn) that were yellow to brownish-red in color with the highest QY reaching 16%.[103] In addition to these preparation methods, carbonization at high temperatures has also been used to prepare Eu^{3+}@ CDs.[104] In summary, metal–CD composites have increasingly attracted more attention in recent years and many studies regarding the synthesis, properties and applications of this type of composite have been reported. Selective examples of metal–CD composite systems are summarized in Table 1.

2.2. Synthesis of nonmetallic inorganics–CD composites

Nonmetallic inorganics–CD composites are another type of composite derived from CDs by compositing with inorganic materials such as ceramics,[107,108] quantum dots (QDs),[109] graphene[110] as well as carbon nanotubes (CNTs).[111,112] Precisely speaking, metals (including metal nanoparticles and metal oxides) as well as the above-mentioned materials (ceramics, QDs, graphene and CNTs) can all be classified as inorganics. Since there have been extensive studies on metal–CD composites, tuning of the optical properties and the application scope of metal–CD composites are quite different from those of other nonmetallic inorganics–CD composites, and thus we provided a separate section for metal–CD composites, which is discussed above. As such, in this section, we will specifically focus on nonmetallic inorganics–CD composites that contain the above-mentioned traditional inorganic materials.

2.2.1. Synthesis of nonmetallic inorganics–CD composites by heteroatom doping. Strictly speaking, heteroatom doped CDs are hardly considered as "composites" of CDs with inorganic materials; however, there has been much work on heteroatom doping of CDs,[113,114] which was very effective in enhancing the properties of CDs. Therefore, we dedicate a short section to discuss heteroatom doping and its effects on CD composites. Heteroatom doping can be divided into single atom doping and multiple atom co-doping. There have been many reports about single-atom doped CDs, including nitrogen,[115] sulfur,[116] boron,[117] phosphorus,[118] silicon[119,120] and fluorine.[121] By introducing atomic impurities into CDs, their electronic structures could be adjusted to generate n- or p-type carriers. As a result, the electronic and optical properties of CDs could be fine-tuned by using specific doping atoms. Single atom doping exhibits great potential in tuning the intrinsic properties of CDs; however, it also has limitations. One of the major limitations is that the emission spectra are generally confined to single atom doped CDs. Therefore, doping of CDs with multiple atoms has attracted much attention, since it could create unique electronic structures due to the synergistic effects from the various doped heteroatoms in CDs.[18] Until now, co-doping of CDs with N/S,[122–125] N/P,[126] N/B,[127,128] N/S/B[129] and N/S/P[130,131] has all been reported.

2.2.2. Synthesis of nonmetallic inorganics–CD composites by compositing with traditional inorganic materials. Depending on the nature of the inorganic molecules, the nonmetallic inorganics–CD composites can be prepared *via* physical mixing, hydrothermal treatment,[132,133] the sol–gel method and microwave irradiation.[134–137]

2.2.2.1. Synthesis via physical mixing. As one of the most widely used ceramic materials, alumina (Al_2O_3) is often used as an adsorbent, a catalyst and a sensor material because of its large surface area, high thermal stability and good mechanical strength.[138,139] Composites of alumina and CDs have been shown to prevent aggregation and improve the thermal stability of CDs, and endow alumina with better PL properties, improving its applications in the optoelectronic field. In most studies, CDs and mesoporous alumina (MA) were prepared individually in advance, and then the two were assembled *via* hydrogen-bonding interactions under simple stirring (Fig. 5A).[140,141] In another study, the MA–CD composites, which were prepared through the same method, demonstrated a much higher fluorescence QY (46.69%) and long-term stability, while the QY of CDs was ~33% and the QY of MA was ~2.11% (Fig. 5B).[142]

QDs derived from semiconductors have attracted much attention in the optoelectronic field because of their unique electronic and optical properties, such as a high extinction coefficient, a high fluorescence quantum efficiency, size-dependent broad absorption, and excellent photochemical stability.[145–147] Recently, they have been composited with CDs to achieve unique properties. For instance, a ratiometric fluorescence sensor was prepared *via* simple mixing and stirring of CDs and QDs for the detection of Hg^{2+} and Cu^{2+}(Fig. 5C).[148] In addition to the above-mentioned examples, CNTs, SiO_2 and GO have also been composited with CDs *via* simple physical mixing (Fig. 5D).[149–151]

2.2.2.2. Synthesis via hydrothermal/solvothermal treatment. Hydroxyapatite (HAp) is a natural mineral form of calcium apatite and the main inorganic component of bone tissues. HAp exhibits good biocompatibility and bone bioactivity, and is thus widely used as a scaffold in bone tissue engineering (BTE).[152,153] Recently, much attention has been paid to the composites of HAp and CDs for applications in the biomedical field, more specifically, BTE.[154–156] Composites of HAp and CDs are mainly prepared *via* hydrothermal treatment, which could produce composites with uniform structures, controlled size and strong interactions between HAp and CDs. Depending on the nature of the precursors, the synthesis of the composites could be carried out *via* four different routes: (1) raw materials of HAp and carbon precursors are treated hydrothermally in a one-pot fashion, and the formation of HAp, and CDs as well as their composite is achieved simultaneously (Fig. 6A);[157,158] (2) HAp is pre-synthesized or readily-made, and then treated hydrothermally with carbon precursors; (3) CDs are pre-synthesized and then treated hydrothermally with raw materials of HAp;[159] (4) both HAp and CDs are synthesized in advance, and then the two are treated together hydrothermally to obtain their composites.[160] In addition to HAp, the composites of CDs

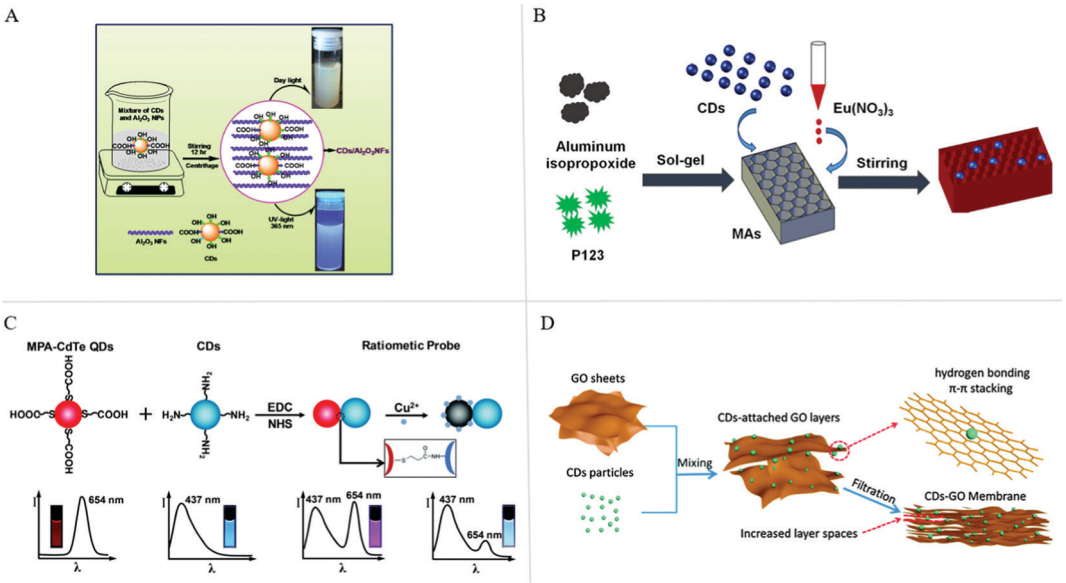

Fig. 5 (A) Schematic illustration of the synthesis process of CDs/Al_2O_3 NFs. Reproduced with permission from ref. 140. Copyright 2020, Elsevier. (B) Schematic illustration of the synthesis process of CD/MA hybrid materials. Reproduced with permission from ref. 142. Copyright 2017, Elsevier. (C) Schematic illustration of the synthesis of the composite derived from carboxyl-modified red fluorescent cadmium telluride (CdTe) quantum dots and amino-functionalized CDs for the determination of Cu^{2+}. Reproduced with permission from ref. 143. Copyright 2016, The Royal Society of Chemistry. (D) Schematic illustration of the fabrication process of CD–GO membranes. Reproduced with permission from ref. 144. Copyright 2014, The Royal Society of Chemistry.

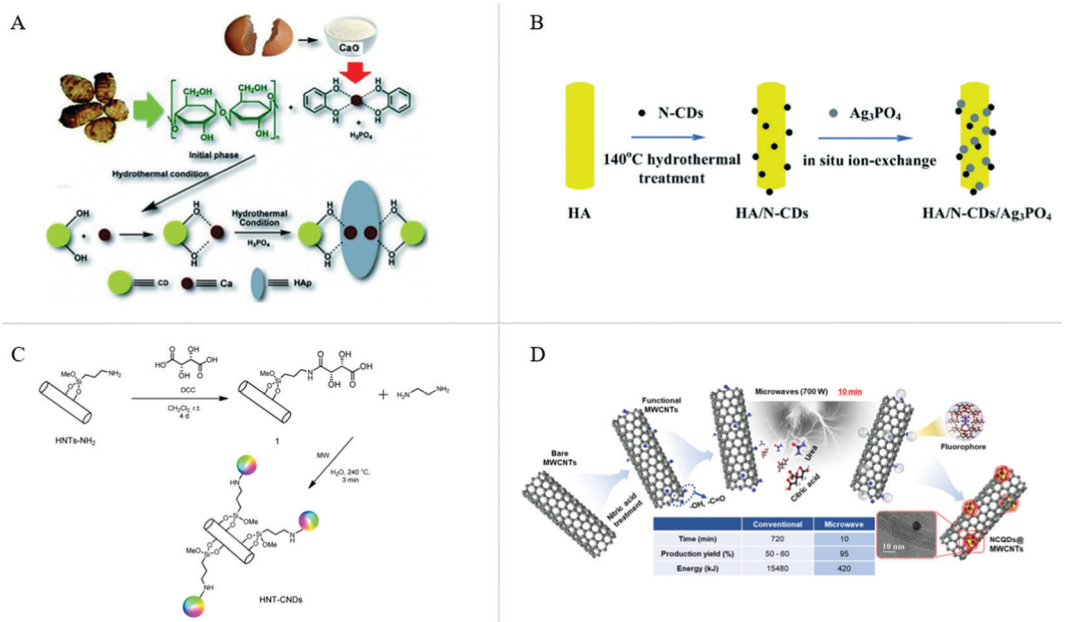

Fig. 6 (A) Schematic illustration of the synthesis process of the CD@HAp nanohybrid. Reproduced with permission from ref. 158. Copyright 2016, The Royal Society of Chemistry. (B) Schematic illustration of the synthesis process of HA/N-CDs/Ag_3PO_4. Reproduced with permission from ref. 172. Copyright 2017, The Royal Society of Chemistry. (C) Schematic illustration of the synthesis process of HNT–CDs. Reproduced with permission from ref. 173. Copyright 2018, The Royal Society of Chemistry. (D) Schematic illustration of the synthesis process of NCQDs@MWCNTs. Reproduced with permission from ref. 174. Copyright 2020, Elsevier.

with other bioceramics (*i.e.*, Si, SiO_2) could also be achieved *via* simple hydrothermal treatment of the two components.[161,162]

Graphene and its derivatives (*i.e.*, graphene oxide) have good physical and chemical properties; however, due to the strong π–π stacking and van der Waals interactions among the sheets, it is common to observe irreversible agglomeration and precipitation in their aqueous solutions, significantly limiting their practical applications.[163,164] Encouragingly, by compositing with

CDs, the aggregation of graphene and its derivatives could be effectively prevented, probably due to the insertion of CDs between the sheets. As a result, their practical applications in biomedical fields are greatly improved.[165] What is more, CDs can function as reducing agents during the composition process, generating CD-reduced graphene oxide (rGO) composites. The CD/rGO hybrids have been demonstrated as efficient probes for the detection of dopamine and acetylcholine, as well as electrocatalysts for electrochemical energy conversion.[166–169] In a different study, Yang *et al.* synthesized an NH_4F–CD composite using citric acid, thiourea and ammonium fluoride by a solvothermal method,[170] in which the emissions of the composite were pushed to the NIR region by the negatively charged, electron-withdrawing F^- which could reduce the bandgap. In addition to these examples, the composites of CDs with other inorganic materials such as NH_2, TiO_2/GO, and HAp/Ag_3PO_4 have also been reported (Fig. 6B).[171,172]

2.2.2.3. Synthesis via other preparation methods. In addition to physical mixing and hydrothermal treatment as mentioned above, there are also some other methods (*i.e.*, microwave-assisted synthesis) for the composition of CDs with inorganic materials. Microwave-assisted synthesis is an augmentation to the solvothermal/hydrothermal technique where microwave is utilized instead of heat.[175] Compared to hydrothermal treatment, it has the advantages of a short preparation time, environment friendliness and low cost. For example, Marina *et al.* synthesized fluorescent halloysite nanotubes (HNTs) by the direct covalent linkage of CDs on the halloysite external surface (Fig. 6C).[173] In another study, CDs were shown to grow on MWCNTs *via* one-step microwave-assisted treatment, and the composites turned out to be promising electrocatalysts (Fig. 6D).[174] In addition to the microwave-assisted method, there were reports showing that CDs@SiO_2 nano-phosphors were synthesized by the reversed-phase microemulsion method and Si–CDs/SiO_2 nanocomposites were generated through a calcination process.[176,177] Selective examples of nonmetallic inorganics–CD composite systems are summarized in Table 2.

2.3. Synthesis of organics–CD composites

Organic materials utilized to compound with CDs include small organic molecules (*i.e.*, folic acid), organic dyes (*i.e.*, Rhodamine B), gels and polymers. Among them, polymers have been the mostly applied organic molecules for compositing with CDs. Compounding CDs with polymers not only enhances the performance of the polymers (*i.e.*, improvising the flexibility, strength, durability, and hydrophilicity),[179] but also passivates the surfaces of CDs to enhance their PL intensity and optoelectronic properties.[180] There are generally three ways in which polymers were used in the preparation of CDs: polymers as direct precursors for CD synthesis, polymers as indirect precursors for CD synthesis, and polymers for CD surface modifications.[51] The last aspect, polymers for CD surface modification/passivation, will be focused on in this section.

2.3.1. Synthesis *via* physical stirring. Physical stirring is normally used in the stepwise synthesis strategy, in which CDs are synthesized in advance before compounding with organics. The stepwise approach for the preparation of organics–CD composites has received significant attention due to its wide applicability and good compounding effect. For instance, modifications with polyethylenimine (PEI) can improve the PL properties and biocompatibility of CDs, since the amino groups of PEI can generate strong hydrogen bonding with organic compounds containing oxygen or nitrogen functional groups. In another example, Han and co-workers synthesized PEI-CDs by simply stirring the mixture of PEI and CDs, and the obtained composite had a QY of 3.5%.[181,182] In addition to polymers, small nitrogen-containing organic molecules such as 2,2′-(ethylenedioxy)bis(ethylamine) (EDA) were also commonly used to passivate CDs, which could enhance the optical properties (Fig. 7A).[183] In these composites under physical stirring, the forces that are responsible for the interactions of CDs and organic molecules were quite different. For instance, in Wu and co-workers' report, negatively charged CDs interacted with tetraplatinated porphyrin (PtPor) to form a composite *via* electrostatic forces,[184] while in another study, a CD-aggregation-induced emission (AIE) composite was formed through

Table 2 Selective examples for the synthesis of nonmetallic inorganics–CD composites

Composite form[a]	Carbon source[b]	Synthesis method[c]	Reaction parameters	Size (nm)	QY (%)[d]	Application[e]	Ref.
CDs/MAs	EDA	PM	8 h	—	46.69	TP	142
CQD@f-MWCNTs	AC	PM	4 h	10–50	—	ES	150
CDs-SiO_2	CA	PM	80 °C, 3 h	84–190	34	Sensor	178
NCQDs/HAp	CA	Hydrothermal	190 °C, 24 h	30–200	31.43	—	157
CD@HAp	CCE	Hydrothermal	170 °C, 15 h	50–80	—	BTE	158
Si–CDs	Tri-SC	Hydrothermal	200 °C, 2 h	3–7	30	Biosensor	161
CDs–SiO_2	APTMS	Hydrothermal	300 °C, 2 h	1–5	42.6	TP	162
CDs@rGO	GO	Hydrothermal	300 °C, 2 h	—	—	Biosensor	166
rGO-CDs	Sucrose	Hydrothermal	90 °C, 4 h	5–15	—	Biosensor	167
HNT-CDs	TTA	Microwave	200 W, 1/20 h	3.3–4.7	17	—	173
CQDs@SiO_2	CA	RPMM	—	18–159	—	LED	176

[a] MAs: mesoporous aluminas; f-MWCNTs: functionalized multi-walled carbon nanotubes; HAp: hydroxyapatite; rGO: reduced graphene oxide; HNT: halloysite. [b] EDA: ethylenediamine; AC: activated carbon; CA: citric acid; CCE: corms of *Colocasia esculenta*; GO: graphene oxide; Tri-SC: trisodium citrate; APTMS: 3-aminopropyltrimethoxysilane; APBA: 3-aminophenylboronic acid; TTA: tartaric acid. [c] PM: physical mixing; RPMM: reversed-phase microemulsion. [d] QY: quantum yield. [e] TP: temperature probe; ES: electrochemical sensor; BTE: bone tissue engineering; LED: light-emitting diode.

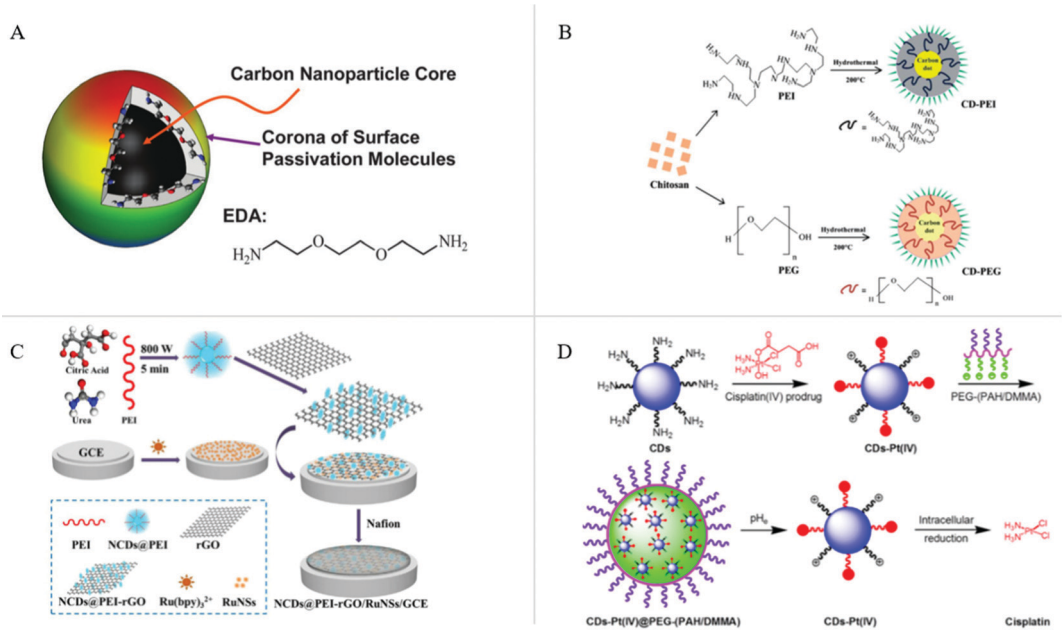

Fig. 7 (A) A cartoon showing the core–shell structure of EDA–CDs. Reproduced with permission from ref. 183. Copyright 2016, The Royal Society of Chemistry. (B) Schematic illustration of the synthesis process of CD-PEI and CD-PEG. Reproduced with permission from ref. 194. Copyright 2014, The Royal Society of Chemistry. (C) Schematic illustration of the construction process for the PEI-N-CD based ECL biosensor. Reproduced with permission from ref. 203. Copyright 2016, Elsevier. (D) Schematic illustration of the synthesis process of CDs–Pt(IV)@PEG-(PAH/DMMA). Reproduced with permission from ref. 56. Copyright 2016, American Chemical Society.

supramolecular assembly of CDs and a hydrophobic AIEgen.[185] In some studies, CDs and organic molecules could be composited *via* covalent bonding under very mild conditions (*i.e.*, stirring at r.t.). For example, the RhB–CD composite was obtained by mixing the solutions of activated CDs and RhB, in which the amino groups of RhB covalently reacted with the carboxyl groups on the CD surface.[186] Similarly, CDs could be facilely conjugated with folic acid (FA) *via* simple crosslinking chemistry.[187,188] The composition of CDs with these organic molecules was extremely useful in enhancing the optical properties of CDs and endowing them with unique properties (*i.e.*, cancer targeting ability).

2.3.2. Synthesis *via* hydrothermal/solvothermal treatment. Considering its environment friendliness and strategy convenience, hydrothermal treatment is also generally used for forming composites of organics and CDs, either *via* one-pot or stepwise synthesis. Polyethylene glycol (PEG) has been widely applied to compound with CDs since a skin layer of PEG may increase the biocompatibility, enhance the photostability, and even cause red-shift in the fluorescence emission of CDs.[189–192] To study the effects of CDs and PEG on the properties of the obtained composites, some research groups have synthesized a series of CDs using different precursors (*i.e.*, TNP and chitosan) using the same preparation method but different reaction conditions and composited with PEG.[193]

Besides PEG, hydrothermally-prepared PEI-CD composites were also frequently reported (Fig. 7B).[194] For instance, Dong *et al.* synthesized branched polyethylenimine (BPEI)-CDs through the low temperature carbonization method. The obtained BPEI-CDs exhibited strong FL activity with a high PL QY (42.5%).[195] Interestingly, in some of these studies it was observed that the fluorescence intensity of PEI-CDs decreased with the increase of solution pH, and thus could be used to develop pH sensors.[196] In addition to these examples, other organics–CD composites such as (N-(2-aminoethyl)-3-aminopropyl)tris-(2-ethoxy)silane-CDs (KH791-CDs), N-isopropylacrylamide-CDs (NIPAAM-CDs), the CD–RhB core–shell nanocomposite and (polyamidoamine)-PAMAM-NH_2-CDs have also been reported.[197–200] It is also worth mentioning that the QY of NIPAAM-CDs was as high as 94%. Interestingly, in hydrothermal reactions, the solvents used for work-up could play important roles. For instance, Lu and co-workers prepared dopamine–CD composites through a one-pot hydrothermal method and the resulting composites were extracted with two different solvents (water and ethanol). Surprisingly, the two dopamine–CD composites exhibited different physical (*i.e.*, solubility) and optical properties: the emission of dopamine–CD composite extracted from ethanol was centered at 710 nm with a QY of 26.28%, while that of the composite extracted from water was centered at 685 nm with a higher QY (33.96%).[201,202]

2.3.3. Synthesis *via* microwave-assisted treatment. Microwave-assisted synthesis is widely used in the preparation of organics–CD composites due to its short reaction time and low cost. Since microwave irradiation can provide high energy in a very short duration, the selection of a suitable reaction time is essential for tuning the properties of the composites formed. For instance, Liu and co-workers synthesized PEI-CDs *via* microwave-assisted treatment and only a specific microwave pyrolysis condition (700 W for 15 min) could result in excellent PL

Table 3 Selective examples for the synthesis of organics–CD composites

Composite form[a]	Carbon source[b]	Synthesis method	Reaction parameters[c]	Size (nm)	QY[d] (%)	Application	Ref.
EDA-CDs	CNP	Stirring	120 °C, 72 h	~5	15–20	Composite films	183
CDs@PtPor	CA	Stirring	R.T., 24 h	6~9	36	Cancer therapy	184
FA-CDs	Dandelion leaf	Stirring	R.T., 24 h	5~8	—	Bioimaging	187
PEG_{6000}-CDs	TNP	Hydrothermal	180 °C, 12 h	51–120	—	Bioimaging	193
BPEI–CQDs	CA	Pyrolysis	<200 °C, 1/3 h	4–10	42.5	Chemical sensor	195
PEI-CDs	EG, PEI	Hydrothermal	180 °C, 24 h	6–10	38	Fluorescence probe	196
KH791-CDs	LasA	Hydrothermal	92 °C, 12 h	3–4	8.6	Solar cells	197
NIPAAM-CDs	CA	Hydrothermal	160/200 °C, 5 h	2–3	94	Bioimaging	198
PEI-CDs	Glycerol	Microwave	700 W,1/12-1/4 h	3–13	7–15.3	Gene delivery, bioimaging	204
RNase A-CDs	CA	Microwave	700 W, 1/15 h	25–45	24.2	Bioimaging	206

[a] BPEI: branched polyethylenimine; EDA: 2,2′-(ethylenedioxy)bis(ethylamine); PtPor: tetraplatinated porphyrin; FA: folic acid; PEG_{6000}: polyethylene glycol 6000; PEI: polyethylenimine; KH791: (*N*-(2-aminoethyl)-3-aminopropyl)tris-(2-ethoxy)silane; NIPAAM: N-isopropylacrylamide; RNase A: ribonuclease A. [b] CA: citric acid; CNP: carbon nanopowder; TNP: 1,3,6-trinitropyrene; EG: ethylene glycol; PEI: polyethylenimine; LasA: L-ascorbic acid. [c] R.T.: room temperature. [d] QY: quantum yield.

performance: a shorter irradiation time led to incomplete surface passivation, while a longer time led to the formation of large particles, both of which resulted in low PL.[204,205] In a different study, the RNase A@CDs composite with a QY of 24.2% was also prepared *via* microwave-assisted treatment.[206] Selective examples of organics–CD composites are summarized in Table 3.

2.4. Synthesis of multi-components–CD composites

Multi-components–CD composites refer to two or more different types of materials composited with CDs. Compared to single-component–CD composites, multi-components–CD composites generally demonstrate better performance (*i.e.*, enhanced fluorescence properties, increased QYs, and expanded application scope).[207–209] For example, a study showed that Mg–CDs and EDA–CD composites had QYs of 18.2 and 73.1%, respectively; however, the multi-component composite Mg–EDA–CDs presented a much higher QY than the two, reaching 83.0%.[210] Despite multi-components–CD composites bearing superior properties, they come with some indelible shortcomings: (1) due to the involvement of multiple components, the preparation of multi-components–CD composites is much more complicated compared to that of single-component–CD composites.[211,212] (2) The characterization of multi-components–CD composites is also much more challenging, and their spectra are generally more complex.[213–215] As a result, studies reported so far regarding multi-components–CD composite fabrications generally focus on the doping effects of different elements from these components composited with CDs.

2.4.1. Synthesis *via* hydrothermal/solvothermal treatment. By compounding with more than one type of material, various elements (atoms) could be introduced into CDs, which can endow CDs with excellent properties (*i.e.*, high QYs and wide emission). Thus, multi-atom co-doped composites have attracted significant attention. Among the elements, N is the most commonly used dopant considering its comparable size and ability to form strong bonds with carbon. On the other side, chelation of metal ions is conducive to the combination of amino and carboxyl groups on CDs through chemical reaction procedures, and thus N- and metal ion-containing materials are commonly composited with CDs.[216] Most of these composites can be achieved *via* simple hydrothermal treatment; for instance, Au, N-CD; Ag, N-CD; Cu, N-CD; Al, N-CD and Mg, N-CD composites have all been reported, in which Mg, N-CDs demonstrated the highest QY of 58.8%.[217–221] Interestingly, the coordination bonds between silver ions and nitrogen atoms can enlarge the band gap of CDs, resulting in enhanced fluorescence emission.[222] In addition to these examples, Fe, Br–CD and N, S-CD–MnO_2 nanocomposites have also been synthesized through simple hydrothermal treatment.[223,224]

2.4.2. Synthesis *via* microwave-assisted treatment. Due to its short preparation time and simple procedure, microwave-assisted synthesis is also commonly applied for the preparation of multi-components–CD composites. For instance, Sai *et al.* successfully synthesized nitrogen and zinc co-doped CDs (N, Zn–CDs) with microwave-assisted treatment (130 °C for 60 min). Interestingly, N, Zn–CDs exhibited bluish-green luminescence with a high QY (74%), while the control sample (N-CDs) displayed blue luminescence with a much lower QY (2.63%). The authors attributed this phenomenon to the presence of oxygen functionalities in the ZnO lattice structure, which might have lowered the energy required for the electronic transitions responsible for the radiation.[225] In addition, synthesis of PEI-N-CD[203] (Fig. 7C) and N, S-CD-P25[226] heterostructured nanocomposites *via* microwave-assisted treatment has also been reported.

2.4.3. Synthesis *via* other preparation methods. In addition to hydrothermal and microwave-assisted synthesis, some other approaches such as physical stirring, ultrasound, and chemical coupling have also been reported for the composites of CDs with more than one type of component.[227] In these approaches, however, it generally requires a separate step to prepare CDs in advance, following which the obtained CDs can then be compounded with other components. For instance, Deng *et al.* prepared a N-CD–AuNP nanosensor by assembling the N-doped CD shell on AuNPs.[228] Tao *et al.* reported a CD–Pt(IV)@PEG-(PAH/DMMA) composite which was based on cisplatin(IV) prodrug-loaded charge-convertible CDs (Fig. 7D).[56]

3. CD composites for biomedical applications

3.1. CD composites for bioimaging

Considering the unique properties of CD composites, such as excellent biocompatibility, outstanding photostability, and low toxicity with multicolor emission, they have been widely applied for bioimaging. Among the various applications, majority of reports focus on fluorescence imaging, while a few present other types of imaging (*i.e.*, photoacoustic imaging).

3.1.1. CD composites for fluorescence imaging. Fluorescence is the most effective tool for tracking the cellular system *in vitro* and *in vivo*, and thus fluorescence imaging has been one of the most common applications of CDs and their composites in recent years. In general, fluorescence imaging requires a certain ability of photon scattering and light absorption from the imaging probe. As a type of luminescent material, CDs have unique PL properties and high QYs, which make them suitable as probes for fluorescence imaging.[229–231] Despite these advantages, CDs also face some challenges, for example, it is generally difficult to access red/NIR emitting CDs and functional CDs with tissue- or cellular compartment-specificity.[232] In this context, heteroatom (*i.e.*, N, S, and P) doping and surface modification are among the most effective means to improve the fluorescence properties of CDs, and thus are commonly applied for all kinds of bioimaging.[233–235]

For most *in vitro* cell imaging applications, CD composites were generally found to accumulate in cell membranes and the cytoplasm (Fig. 8A),[236–238] and only a few examples demonstrated the ability to enter and image the nucleus.[239,240] To enhance the imaging specificity of CDs, it is a common practice to conjugate additional targeting moieties. For instance, Wu and co-workers reported PEI-ML-CDs, which could specifically target and image lysosomes due to the presence of the

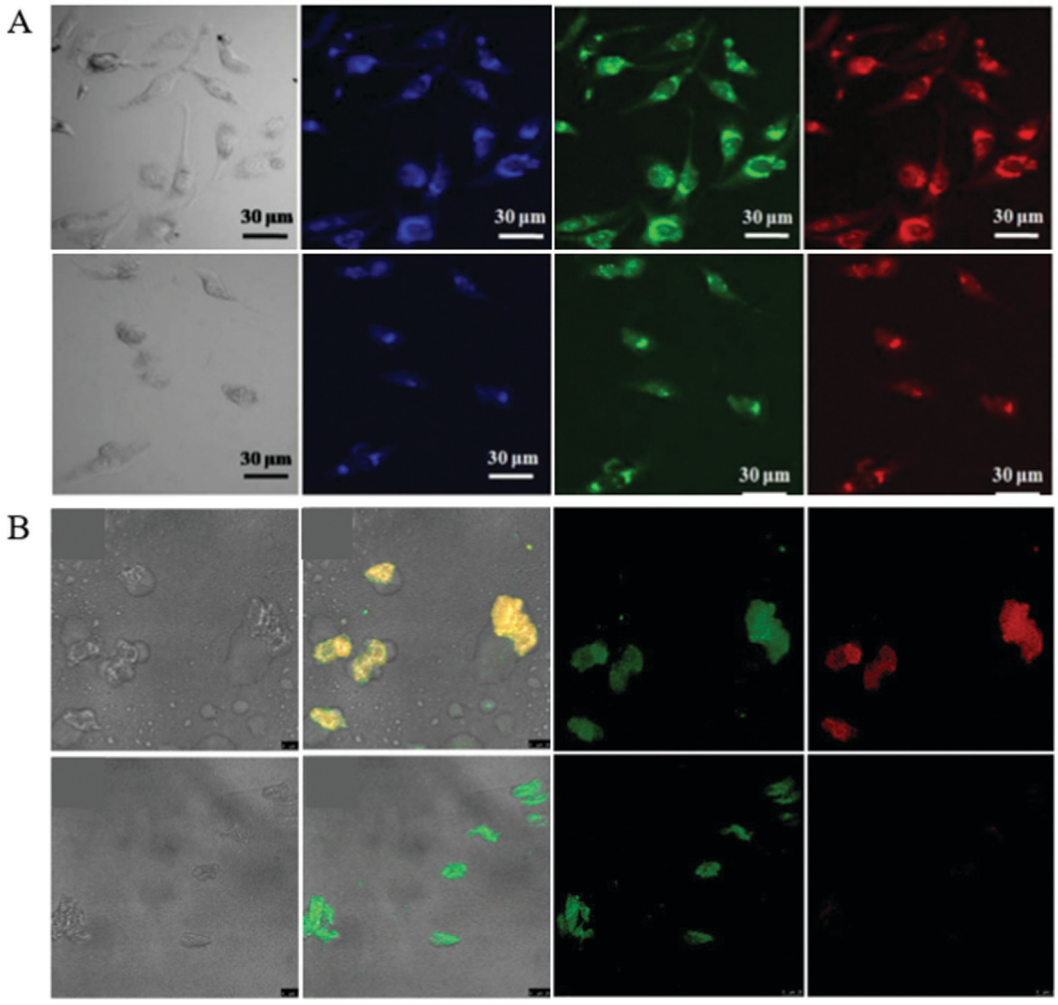

Fig. 8 (A) Laser scanning confocal microscope (LSCM) images of 786–0 cells incubated with 0.30 mg mL^{-1} N-CDs/10 mM Fe^{2+} (top) and Fe^{3+} (bottom). The first, second, third and fourth panels are cell images taken of the bright field, 405/422 ± 25, 488/500 ± 25, and 543/650 ± 25 nm ($\lambda_{ex}/\lambda_{em}$), respectively. Reproduced with permission from ref. 236. Copyright 2014, Elsevier. (B) Fluorescence images of MC3T3-E1 cells incubated with Au–CDs in the absence (top)/presence (bottom) of 30 μM Fe^{3+}. The first, second, third and fourth panels are cell images taken from the bright-field, overlay of fluorescence images, blue channel and red channel. Reproduced with permission from ref. 247. Copyright 2016, American Chemical Society.

morpholine group.[241] Lu *et al.* reported dopamine–CD composites which could penetrate the cell membrane and distribute in the cytoplasm region in AGS and K562 cells.[202] In addition, Zhang *et al.* synthesized CD–AIE through supramolecular assembly of CDs and a hydrophobic AIEgen. The CD–AIE exhibited superior imaging ability *in vivo* and could act as an ideal fluorescent probe for noninvasive long-term tracing and imaging applications.[185]

Multiplex fluorescence imaging exhibits the advantage of detecting multiple emissions from a single fluorescent source, and thus the images have higher resolution.[242] Recently, applications of CD composites in multiplex fluorescence imaging have been reported.[243–246] Zhang and co-workers synthesized Au–CDs and successfully applied this system for ratiometric fluorescence imaging to monitor the Fe^{3+} level in cells, in which both blue and red channels were excited under single excitation (Fig. 8B).[247] Fe^{3+} can significantly quench red fluorescence by combining with the COOH and NH_2 groups on the surface of Au–CDs; however, the change of blue fluorescence is very small. With the addition of 30 μM Fe^{3+} to osteoblast cells after 10 h, the fluorescence of the red channel was almost quenched; however, there was almost no change in the blue channel. To explore the interactions of M@CDs (M: Ag, Au, Ga, Sn and Zn) with neurons, Vijay *et al.* co-cultured M@CDs with PC12 cells and the images showed the differentiation progress of the cells at different time intervals, which demonstrated the potential application of M@CDs in neural tissue engineering.[103] Furthermore, by compounding CDs with specific small molecules, CD composites could exhibit unique properties. For instance, FA can bind to the folate receptors on the surface of cancer cell membranes and then enter cells *via* receptor-mediated endocytosis with non-immunogenicity.[248] Zhao *et al.* reported FA@CDs for specific anchoring to the nucleus of MCF-7 cells and the cytoplasm of HepG2 cells.[249] The confocal laser scanning microscopy images showed receptor-mediated endocytosis, the expression level of FR, and target recognition of cancer cells of the fluorescent FA–CDs. Furthermore, FA@CDs were further applied for nucleus-targeting photodynamic therapy (PDT) in H413 cells, and the results showed that FA@CDs could function as targeting and delivery agents, and thus enhanced the PDT efficiency.[250]

For *in vivo* fluorescence imaging, CDs are expected to emit light with long wavelengths; however, most CDs are often emitted in the blue or green region.[251] Therefore, it is very meaningful to obtain a yellow or red emitting CD composite and apply it in *in vivo* fluorescence imaging.[252–254] For instance, Cui *et al.* injected red emitting CDs (R-CDs) into mice intravenously and observed red fluorescence scattering throughout their bodies. Considering tumor cells specifically recognize folic acid, the authors also prepared a folic acid @R-CDs nanomaterial composite. After injecting folic acid@R-CDs into tumor-bearing nude mice for 24 h, the images showed that red fluorescence concentrated at the tumor site and positively correlated with the concentration of the composite (Fig. 9A–D).[255] In a different study, Lu and co-workers injected dopamine–CD composites into the back of a mouse and a strong fluorescence signal was observed when excitation and emission wavelengths were 540 and 600 nm, respectively.[201] Among the CD composites applied for *in vivo* fluorescence imaging, there are also many reports on N-doped CDs.[256] In addition, PEI and polydopamine (PDA) modified CDs have also been reported and achieved excellent *in vivo* fluorescence imaging (Fig. 9E–H).[257,258]

3.1.2. CD composites for non-PL imaging. As discussed above, fluorescence-based imaging techniques for *in vivo* imaging applications are sometimes restricted due to the limited tissue penetration depth and tissue autofluorescence interference. To bypass these restrictions, photoacoustic (PA) imaging has been developed, making imaging above the optical diffusion limit feasible through the integration of optical excitation with

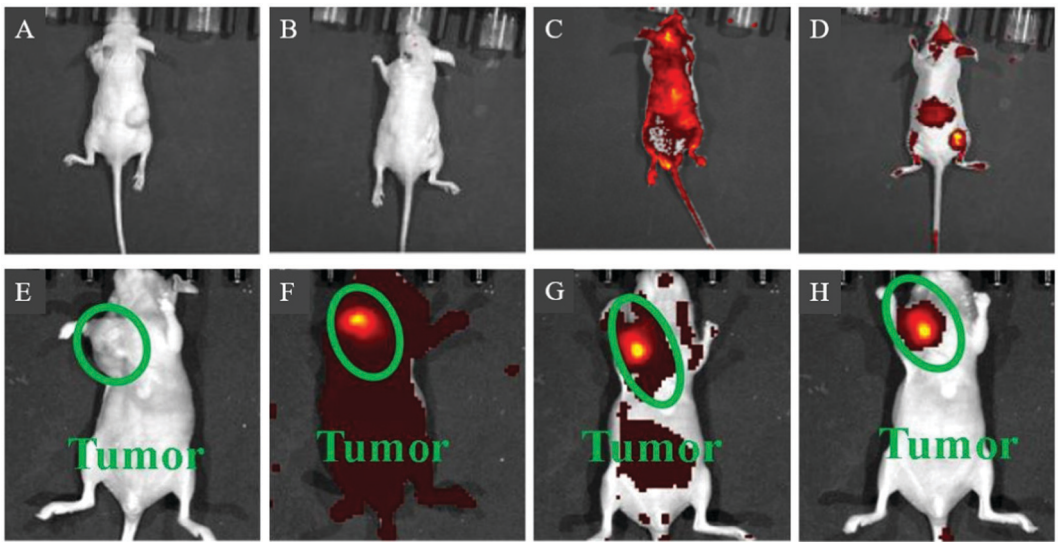

Fig. 9 *In vivo* fluorescence images of HepG2 tumor mice after intravenous injection of (A) saline, (B) folic acid, (C) R-CDs, and (D) folic acid@R-CDs. Reproduced with permission from ref. 255. Copyright 2019, American Chemical Society. *In vivo* fluorescence images of nude mice after intravenous injection of PDA@N-CDs (Mn) NPs in nude mice for (E) 0, (F) 3, (G) 6, and (H) 12 h. Reproduced with permission from ref. 258. Copyright 2019, Elsevier.

ultrasonic detection based on the PA effect. Compared to fluorescence imaging, PA imaging could provide deeper tissue-imaging penetration and higher spatial resolution, which are very suitable for real-time and noninvasive diagnosis of diseases.[259] As such, CD composites (N-CQDs, GNR@SiO_2–CDs) with high photostability and strong absorption in the near-infrared region (NIR) have been developed and applied for non-invasive PA imaging.[260,261] For instance, P, N-CQDs were used as both PA and fluorescence imaging agents for cancer diagnosis.[262] The P, N-CQDs showed dual wavelength emissions in the green and red regions where QYs were 30% and 78%, respectively. The results revealed that P, N-CQDs were taken up by RAW 264.7 cells and mainly incorporated into the cytoplasm region surrounding the nucleus. The PA images of the tumors showed that P, N-CQDs extravagantly accumulated in the tumor and preserved relatively constant PA signals after extended circulation in blood vessels during the whole imaging process (Fig. 10A). The organs and tissues were removed and imaged (Fig. 10B), and the results showed that the tumor and liver tissue exhibited a high fluorescence intensity (Fig. 10C). Otherwise, the intensities of the tumor increased with time after injection, and the green emission reached maxima at about 3 h post-injection and the red emission at 6 h (Fig. 10D).

In addition to PA imaging, magnetic resonance imaging (MRI) is another commonly used imaging technique with excellent sensitivity and high spatial resolution. MRI is regarded as one of the most powerful techniques in modern diagnostic medicine, which has the advantages of high spatial resolution and absence of X-ray radiation, providing anatomical details and high quality three-dimensional images of soft tissue in a non-invasive monitoring manner.[263] Due to their excellent magnetic properties and contrast efficiency, Fe^{2+}, Mn^{2+}, and Gd^{2+} are commonly used as MRI contrast agents.[264,265] However, the deposition of these metal ions *in vivo* causes biosafety concerns, limiting their practical applications for *in vivo* imaging.[266,267] Excitingly, studies showed that doping these ions on CDs could effectively reduce their leakage to a great extent, increase their longitudinal relaxation rate, and show a better magnetic resonance effect.[268–270] For instance, systems based on Gd–CD and Mn–CD composites have been developed and applied as MRI probes, respectively.[271,272] For the Gd–CDs as the MRI probe, it was observed that Gd–CDs were quickly excreted by the kidneys and accumulated in the bladder after 30 minutes of intravenous injection into the mice (Fig. 11A).[273] In another report, the T1-weighted images of Gd@C-dot-Cys-ZEGFR:1907 in HCC827 tumor xenograft nude mice models showed that SBR/SBR0 at 1 h after injection was higher than that before and 2 h or 4 h after injection (Fig. 11B).[274] Zhao *et al.* also reported a Gd/Yb@CDs composite with excellent photostability and MRI signal. Interestingly, this composite could accumulate at the tumor area through free tumor vessels with enhanced permeability and retention, making it a potential cancer diagnosis sensor through MRI imaging (Fig. 11C).[275]

CDs are known to have many superior properties, such as excellent PL properties, high biocompatibility as well as economic and easy accessibility. These unique properties render them excellent candidates for fluorescence imaging agents. However, due to the very nature of CDs (*i.e.*, broad size distribution and non-magnetism), their applications in bioimaging

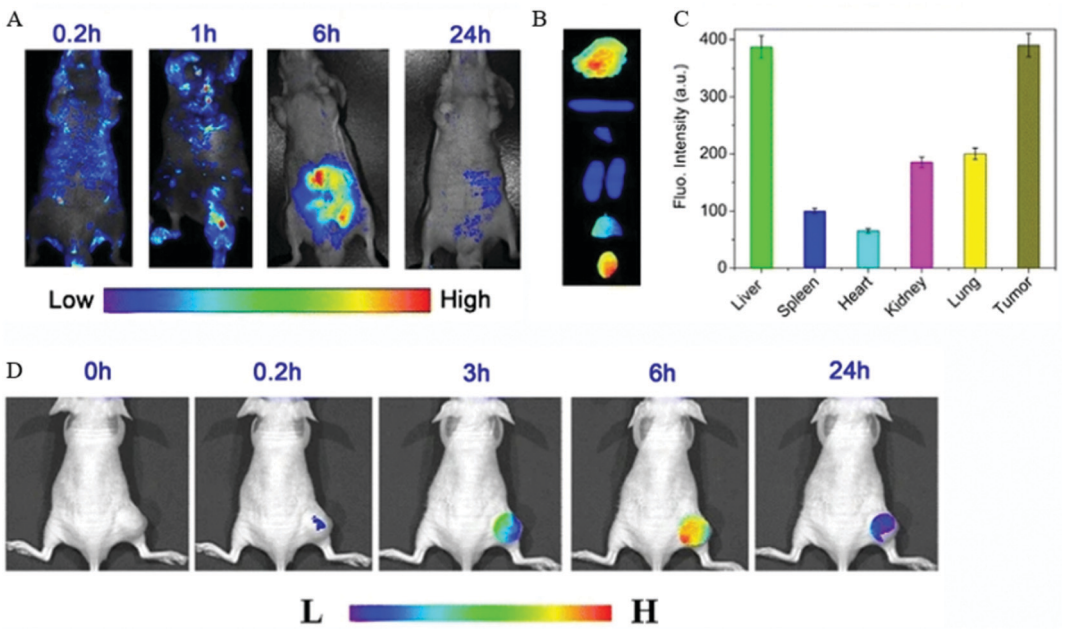

Fig. 10 (A) *In vivo* PA images after intravenous injection of P, N-CQDs in nude mice for different times. (B) *Ex vivo* images of mice tissues from top to bottom: the heart, liver, spleen, lungs, kidneys, and tumor. (C) Fluorescence intensity graph of different mice tissues after intravenous injection of P, N-CQDs. (D) *In vivo* PA images of nude mice after intravenous injection with P, N-CQDs for different times. Reproduced with permission from ref. 262. Copyright 2017, Springer Nature.

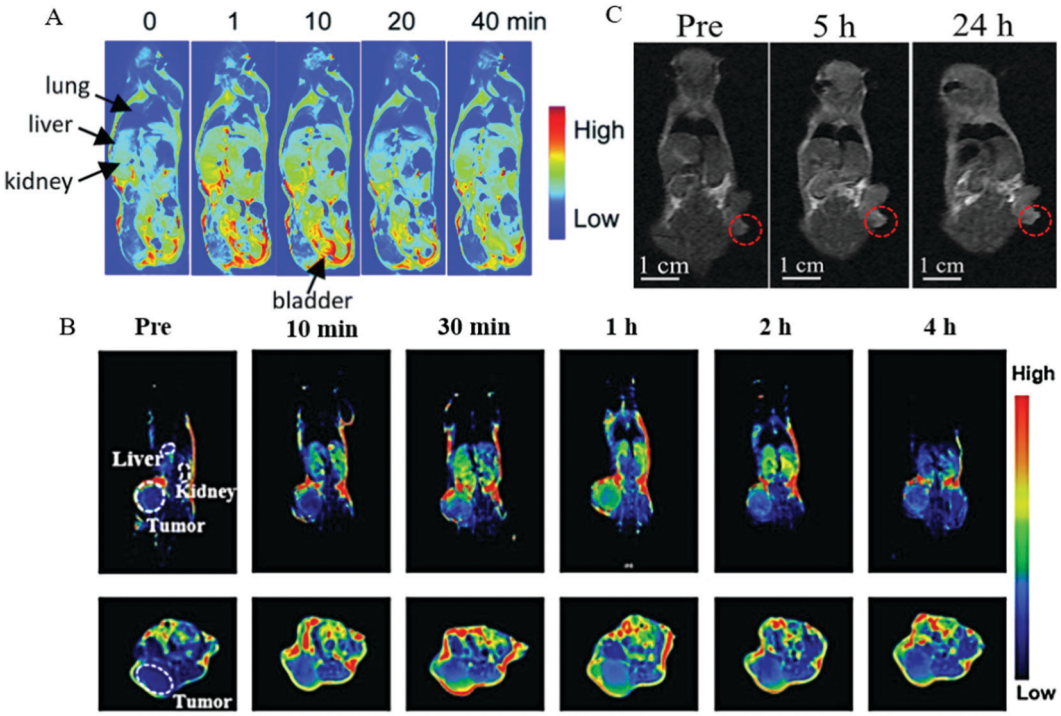

Fig. 11 (A) *In vivo* T1-weighted MR images of mice after intravenous injection of Gd–CDs for different times. Reproduced with permission from ref. 273. Copyright 2015, The Royal Society of Chemistry. (B) *In vivo* MR images of HCC827 tumors in mice after intravenous injection of Gd@CDs-Cys-ZEGFR:1907 for different times. Reproduced with permission from ref. 274. Copyright 2020, The Royal Society of Chemistry. (C) *In vivo* MR images of mice after intravenous injection of Gd/Yb@CDs for different times. Reproduced with permission from ref. 275. Copyright 2018, American Chemical Society.

are generally limited to PL imaging. As discussed above, the applications of CDs in bioimaging could be greatly extended (*i.e.*, PA imaging and MRI) *via* compositing with other materials. Thus, the continuous pursuit of CD-derived composite materials is of great importance for further development of CD-based bioimaging applications.

3.2. CD composites for drug delivery

Due to their small size, high surface area, excellent fluidity, biocompatibility, easy surface functionalization and intrinsic fluorescence properties, CDs have potential for application in the construction of drug delivery systems (DDS). CDs can not only transport drugs into cells, but also serve as a bioimaging agent for tracking drugs. The doping of metal/non-metal ions and surface functionalization could further promote the properties of CDs, increasing the applicability of CD composites in drug delivery related applications.

3.2.1. CD composites for anti-cancer drug delivery. Doxorubicin (DOX) is a commonly used anticancer drug for curing tumors, and it functions by breaking the DNA chain for replication and thus prevents the helix from being resealed, thereby stopping the process of tumor replication.[276] However, due to the nonspecific drug administration, chemotherapy (treatment of cancer using chemicals such as DOX) generally faces significant challenges due to side effects. As such, various CD composites have been tested to improve treatment accuracy and avoid drug side effects by designing and constructing structures and functions together with diagnostic, self-targeting, and drug-delivery functions in anticancer treatment.[277,278] In DDS construction, DOX could be attached to CDs or their composites *via* π–π stacking interactions, weakening the fluorescence of CDs through the fluorescence resonance energy transfer (FRET) mechanism.[279–281] After being delivered to tumor cells, DOX could be released from CDs or their composites upon proper stimulation (*i.e.*, pH change, light excitation, *etc.*), killing cancer cells specifically and effectively.[282] This process could also restore the fluorescence of CDs that was previously quenched, the phenomenon of which could be used to track the location of DOX.

Among the various reports, N-CDs were often combined with DOX for anticancer drug delivery (Fig. 12A).[283] For instance, Gong *et al.* reported N-CDs as a nanocarrier for cancer therapy, which exhibited high quality single- and two-photon fluorescence (QY = 45%), realizing the real-time monitoring of the endocytosis, intracellular distribution and release of DOX (Fig. 12B).[284] In addition, metal– and organics–CD composites were also used to combine with DOX as the DDS.[285–290] For instance, Yao *et al.* prepared magnetofluorescent CQDs (MFCQDs) using a combination of waste crab shell and three different transition-metal ions (Gd^{3+}, Mn^{2+}, and Eu^{3+}) by microwave-assisted pyrolysis. These composites could integrate with DOX and specifically target cancer cells *via* the overexpressed folate receptors.[291] Other groups have synthesized CD conjugated HAp nanocomposites and applied them simultaneously for PL imaging and DOX delivery (Fig. 12C).[292] In these

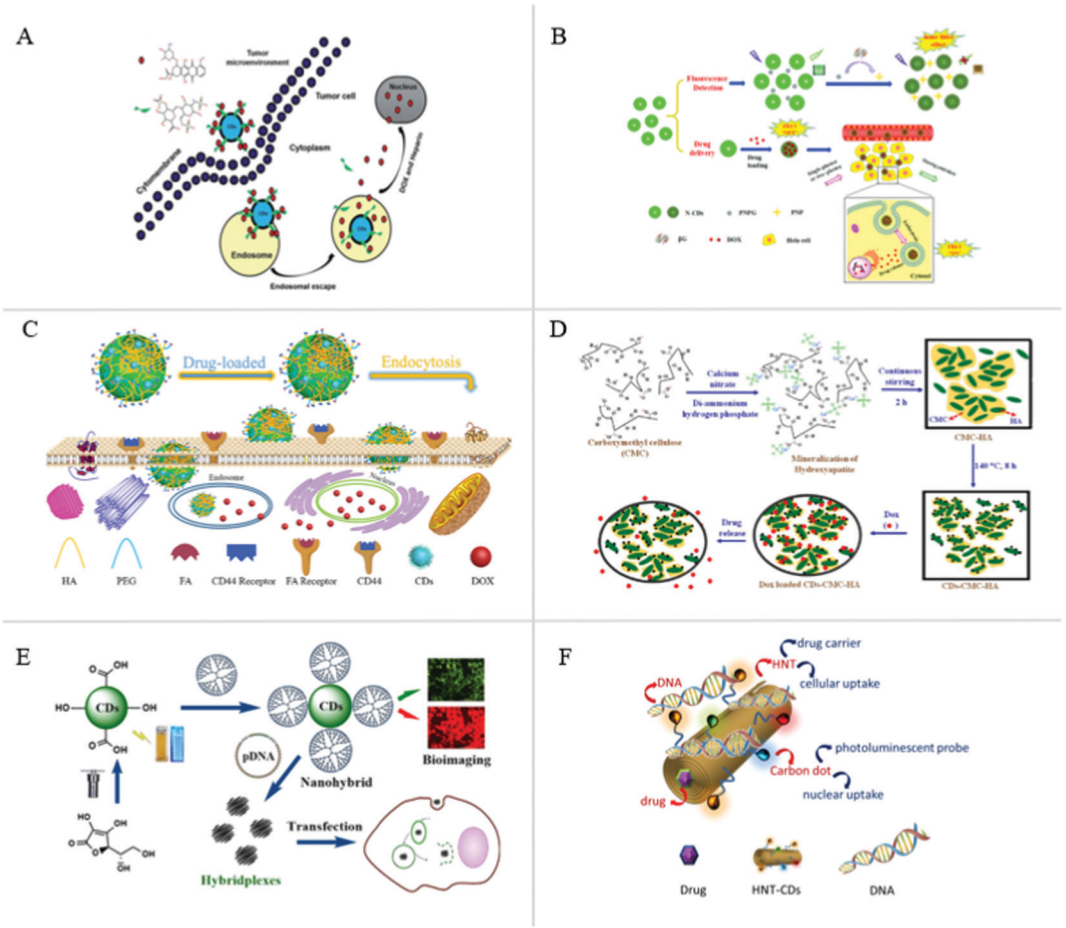

Fig. 12 (A) Illustration of the intracellular release behavior of DOX from the CDs–heparin/DOX drug delivery system. Reproduced with permission from ref. 283. Copyright 2017, The Royal Society of Chemistry. (B) Illustration of the intracellular release behavior of DOX from the N-CDs/DOX drug delivery system by two-photon fluorescence imaging. Reproduced with permission from ref. 284. Copyright 2018, Elsevier. (C) Illustration of the intracellular release behavior from the DOX-loaded FA-PEG-HAp-CD theranostic nanogels. Reproduced with permission from ref. 292. Copyright 2016, Elsevier. (D) Schematic illustration of the intracellular release behavior of DOX from CD decorated carboxymethyl cellulose–HAp nanocomposite (CDs-CMC-HAp). Reproduced with permission from ref. 293. Copyright 2017, Elsevier. (E) Representation of the preparation of CDs@PAMAM nanohybrids and their application for bioimaging and gene delivery. Reproduced with permission from ref. 199. Copyright 2021, American Chemical Society. (F) Cartoon representation of HNT-CD multifunctional nanocarriers. Reproduced with permission from ref. 294. Copyright 2019, Elsevier.

nanocomposites, CDs were synthesized through the *in situ* mineralization and carbonization of HAp. It is worth noting that DOX molecules were loaded through electrostatic interactions with carboxyl groups and eventually released through a diffusion-controlled mechanism (Fig. 12D).[293]

Paclitaxel (PTX) is another commonly used anticancer agent, which can affect nuclear morphology and promote apoptosis through interacting with microtubule polymers and restraining the dissociation of tubulin.[295,296] Gomez *et al.* synthesized N-CDs by a microwave-assisted method and constructed a DDS by coupling these CDs with PTX *via* a carbodiimide condensation reaction. In this DDS, PTX could be readily released from N-CD carriers after internalization due to the hydrolysis of the ester bond between PTX and N-CDs.[297,298] Unfortunately, unlike in other reports, the anticancer efficiency of PTX conjugates was not better than that of free PTX, but they held similar efficiencies. Metronidazole (MET), as an antibiotic, can cause strand damage to the bacterial DNA through the reduction of its nitro-group by an electron transport protein.[299] Madadi *et al.* reported that conjugated cCQD-MET could rapidly internalize into H413 cells and exhibit enhanced antimicrobial activity.[300] In a different study, the CDs@PtPor composite demonstrated strong photocytotoxicity under light irradiation and therapeutic efficacy as well as low side effects *in vitro*, which was developed as a drug nanocarrier in cancer therapy.[184]

3.2.2. CD composites for gene delivery. In addition to antitumor drug delivery, there has also been significant interest in the application of CD composites for gene delivery.[301,302] Gene delivery is the process of introducing foreign DNA into host cells[303] and could be regarded as a special case of "drug" delivery. Gene delivery is one of the necessary steps required for gene therapy and genetic modifications.[304] Gene delivery systems could protect genetic materials from premature degradation during the systemic blood circulation and effectively transport therapeutic genes to the target cells.[305] CDs are

extremely suitable for gene transmission due to their rich surface functionalities. Firstly, the abundance of surface functionalities endows CDs with excellent water solubility; secondly, one can engineer the surface functional groups of CDs so that the loading and release of gene therapeutics could be precisely controlled through the interactions (*i.e.*, covalent interaction) of the two.[306–308] Among various CD composites, PEI–CD composites have been paid much attention due to their synthetic maneuverability and high DNA-binding ability.[309–311] For instance, both Dou and Liu's groups have reported PEI functionalized CDs applied for DNA delivery.[204,312] It is worth mentioning that, in these systems, PEI molecules played two roles: (1) as the surface passivation agent to enhance the fluorescence of CDs and (2) as the polyelectrolyte to condense DNA through electrostatic interactions. Further, PEI-CDs have also been composited with folic acid/hyaluronic acid/fluorine/nitrogen and applied for gene delivery.[313–316] In addition, Ivo *et al.* reported (polyamidoamine)-PAMAM-NH_2-CD nanohybrids for DNA delivery. The nanohybrids showed mild cytotoxicity and presented very high transfection efficiencies (Fig. 12E).[199] Marina and co-workers established a CDs@HNT-DNA model through electrostatic interactions between CDs@HNT and DNA. The results showed that the model did not cause any alteration in the DNA structure and DNA was slowly released through a dialysis membrane in physiological media (Fig. 12F).[294]

3.3. CD composites for optical biosensing

Biosensors, including enzymatic sensors, immunosensors, and nucleic acid sensors, are analytical devices used to detect important organic or inorganic molecules in organisms, which combine biological components with physicochemical detectors.[317,318] Recently, applications of CDs and their composites in biosensing have been widely investigated.[319] Thanks to the unique properties of CDs, sensors derived from CDs and their composites demonstrate various advantages: (1) tunable PL emissions, which render the sensors with superior optical sensing abilities; (2) excellent PL stability, which could avoid many analysis errors caused by the degradation of fluorescent probes; (3) extremely low toxicity of the sensors due to the very nature of CDs (*i.e.*, carbon composed), which warrants their eventual *in vivo* applications; (4) abundance of surface functionalities in the CD composites, which can provide abundant binding sites for specific bioreceptors that are an essential part in the biosensing process; and (5) most importantly, by composition with other materials, sensors derived from CDs could demonstrate high sensitivity and selectivity towards some specific detection objects (*i.e.*, enzymes and nucleic acids).[320–322] Therefore, studies focusing on combining CDs with various materials for the development of CD composite-derived sensing systems have been widely reported.

Optical sensors are among the most investigated CD composite-derived systems. In such a typical optical biosensor, specific targets could be bound to CD composites and recognized by bioreceptors. During this process, interactions of target analytes and CD composites could interfere with the optical signals of CD composites; by monitoring the changes of the optical signals, information (*i.e.*, concentrations) regarding the target analytes could be obtained. Generally speaking, based on their sensing mechanisms, sensors can be divided into three classes, namely "on–off", "on–off–on" and "off–on–off" (Fig. 13).

The type of "on–off" sensors relies on the decrease (or even complete quenching) of CD composites' PL to detect the target analytes. In other words, by developing a negative correlation between the PL intensity of CD composites and the concentration of the target analyte, the concentration of an unknown sample could be calculated from the calibration curve developed (Fig. 13A). Currently, various mechanisms have been elucidated. Among them, three main mechanisms for PL quenching, namely Förster resonance energy transfer (FRET),[323–325] photoinduced electron transfer (PET)[326–328] and inner filtering effect (IFE),[329–331] have been widely used for the design and development of CD composite-based optical biosensors. On the other hand, in a typical "on–off–on" biosensor, the optical signal

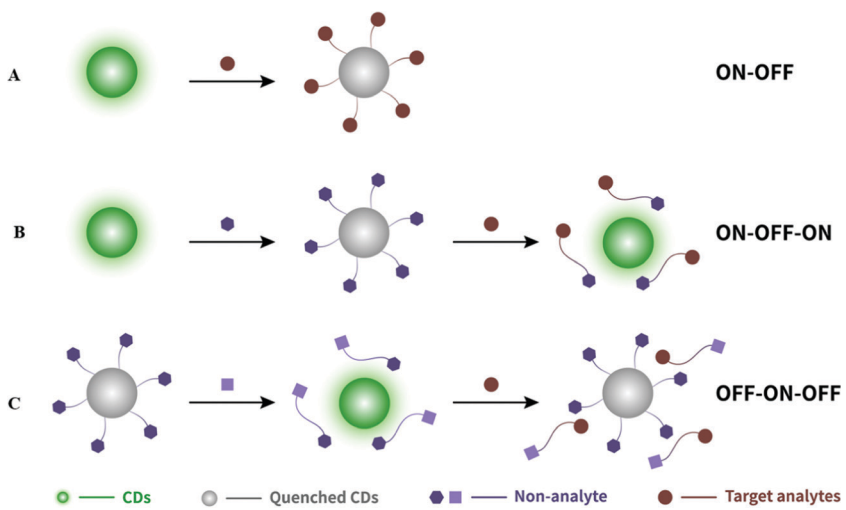

Fig. 13 Cartoon representation of typical optical biosensing strategies: (A) "on–off" strategy; (B) "on–off–on" strategy; and (C) "off–on–off" strategy.

of CD composites undergoes a stepwise change: the PL is first turned off due to the interaction with a non-analyte quencher, then it could be restored in the presence of the target analyte; thus, the degree of recovery of the PL of the CD composites could be used for the detection and determination of the target analyte (Fig. 13B).[332,333] Although uncommon, a sensing platform based on the "off–on–off" strategy has also been reported,[334] in which the quenched PL could be restored due to the interaction with a non-analyte, then the PL could be turned off again in the presence of the target analyte (Fig. 13C). With these sensing strategies, CD composite-derived sensors have been widely developed and achieved great success in the detection and determination of substances such as biologically important molecules,[335–337] and substances of environmental concern[338] as well as metal ions.[339–341]

3.3.1. CD composites for the sensing of biologically important molecules. There are many biologically important molecules closely related to our health, and their presence in proper concentrations is essential for body functions. Thus, it is important to develop facile and reliable sensors to monitor these molecules.[342,343] Glutathione (GSH) and cysteine (Cys) are such molecules that could prevent reactive oxygen species from destroying cellular components. Following the "on–off" strategy, Wu *et al.* established a fluorometric nanoprobe with N-doped CDs for the sensitive detection of GSH, in which the PL of CDs was in a reverse relationship with the concentration of GSH due to the thiol group triggered IFE.[344,345] On the other hand, Cai and co-workers designed novel "on–off–on" biosensors using CD–MnO_2 nanocomposites for the sensing of GSH.[346,347] In this system, the PL of CDs was initially quenched by MnO_2 nanosheets through energy transfer between the two; in the presence of the target analyte GSH, the MnO_2 nanosheets were reduced to Mn^{2+} ions, causing the release of CDs and restoration of CDs' PL (Fig. 14A).

Alkaline phosphatase (ALP) in serum is another biologically important molecule, which is closely related to various diseases including cancer and bone disease; therefore, the sensitive detection of ALP is also of great importance.[348] As such, Li *et al.* established a sensing platform with N-doped CDs (QY = 49%) for the quick and sensitive detection of ALP. In this system, CDs were presented together with *p*-nitrophenylphosphate (PNPP), a substance that could be transformed into *p*-nitrophenol (PNP) under the catalysis of ALP. Since the emission of CDs and the absorption of PNP overlap very well, the PL of CDs could be effectively quenched through the IFE by PNP, thus realizing the sensing of ALP.[349]

In addition to the molecules discussed above, nucleic acids are another class of biologically important molecules; as a result, sensing platforms designed for the detection of nucleic acid based on CD composites have also been extensively studied.[350,351] For instance, Somaye *et al.* developed an ultrasensitive homogeneous biosensor for the detection of HIV-related DNA sequences, the sensing of which was realized by the FRET between CDs and AuNPs.[352,353] Interestingly, the PET mechanism was also adopted to detect DNA using CdTe–CDs as the probe and mitoxantrone as the "on–off–on" signal reagent.[354] In addition to the above examples, the sensing of other biologically important molecules such as ATP, trypsin, dopamine, glucose and RNA has also been successfully realized using CD composites as probes.[355–363]

3.3.2. CD composites for the sensing and substances of environmental concern. Organophosphorus compounds (OPs)

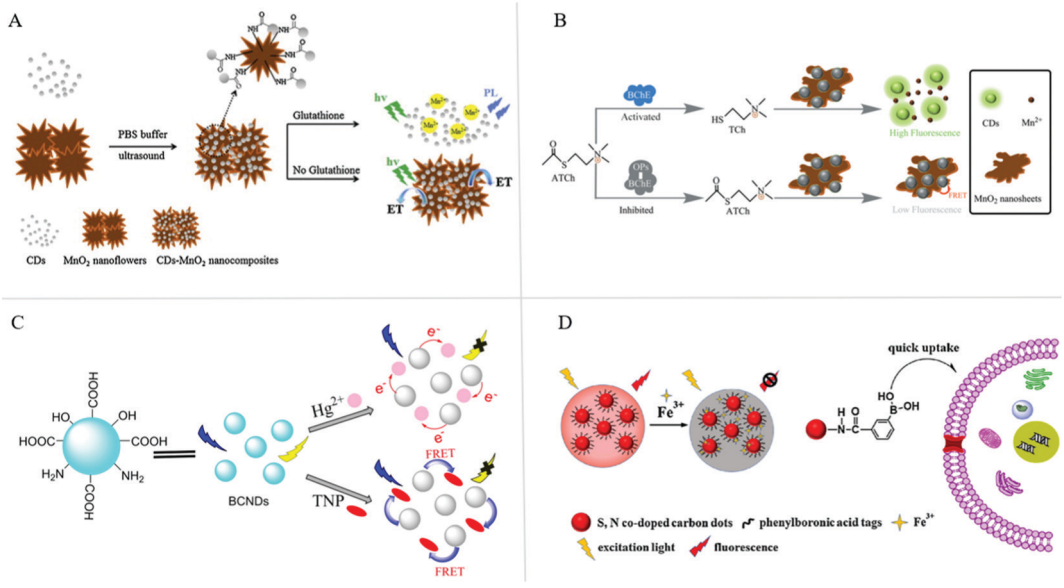

Fig. 14 (A) Schematic illustration of CD–MnO_2 nanocomposites for GSH detection. Reproduced with permission from ref. 347. Copyright 2015, Elsevier. (B) Schematic illustration of CD–MnO_2 nanosheets for OP detection ("off–on–off" strategy). Reproduced with permission from ref. 334. Copyright 2018, American Chemical Society. (C) Schematic illustration of N, B-doped CDs for sensing Hg^{2+} and TNP. Reproduced with permission from ref. 364. Copyright 2016, Elsevier. (D) Schematic illustration of N, S-CDs-PBA for sensing Fe^{3+} in PC12 cells. Reproduced with permission from ref. 365. Copyright 2018, Elsevier.

are the most widely used pesticides in modern agriculture. Due to their strong inhibitory effects on cholinesterase, they are a significant threat to human health. Therefore, attempts to detect OPs with CD composite-based sensors have been frequently made.[366–369] For instance, Hou *et al.* developed a system based on quaternized CDs (Q-CDs) for the detection of dichlorvos. In this sensing system, the detection of the analyte was realized through a FRET process, in which the 5-thio-2-nitrobenzoic acid (TNB) anion acted as the energy acceptor, while Q-CDs acted as the energy donors. The sensor was based on Ellman's test: acetylcholinesterase (AChE) can catalyze the formation of TNB, which can quench the fluorescence of Q-CDs, and dichlorvos can inhibit the activity of AChE, which can recover the fluorescence of Q-CDs, forming the ''on–off–on'' sensor.[370] Following the same mechanism, Yan *et al.* developed an ''off–on–off'' fluorescence platform for the sensitive detection of OPs by utilizing a MnO_2–CD nanosensor[334] (Fig. 14B). Specifically, the quenched PL of CDs by MnO_2 nanosheets through FRET was first recovered by adding butyrylcholinesterase (BChE) and acetylthiocholine (ATCh). However, the BChE activity could be significantly inhibited in the presence of OPs, causing the PL of CDs to be quenched again, and thus realizing the detection of OPs. It is worth mentioning that MnO_2 nanosheets served not only as the nanoquencher but also as the recognition unit for OPs in this sensing platform.

Known as picric acid, 2,4,6-trinitrophenol (TNP) is a general precursor for the production of fireworks, explosives and dyes with a low safety factor and strong explosive ability.[371] Thus, the accurate and sensitive detection of TNP is also very important.[372,373] To detect TNP, Ye *et al.* developed a TNP sensing platform using N, B-doped CDs. This system demonstrated high sensitivity towards TNP, and the limit of detection was 0.35 μM (Fig. 14C).[364] Exploiting a similar sensing mechanism, Wang *et al.* also developed a platform using mesoporous SBA-15 functionalized with 3-glycidyloxypropyltrimethoxysilane and multi-hydroxyl CDs as the probe with a limit of detection down to 0.17 μM.[374] Interestingly, (3-chloro-2-hydroxypropyl)-trimethylammonium chloride functionalized CDs synthesized by Gao *et al.* had a much lower detection limit down to 70.4 nM.[375] In addition to the above-mentioned substances, other molecules of environmental concern such as drugs, tetracycline, H_2O_2, and H^+ (pH) have also been successfully detected and determined by CD composite-based sensing platforms.[376–382]

3.3.3. CD composites for the sensing of metal ions. Metal ions play important roles in various physiological activities and are essential chemicals for all lives. Therefore, sensing methods for the highly sensitive and selective detection of metal ions in biological systems are highly desired. As such, there have been many studies focusing on the applications of CD composites as fluorescent probes for metal ion detection.[383,384] Generally speaking, most of the sensing platforms for the detection of metal ions were designed by following the ''on–off'' strategy.[385,386] When interacting with CD composites, the empty d or f orbitals of the metal ions could host the energized electrons from the excited states of CDs, and thus effectively quench the PL of CDs through PET. As a result, most of the sensing platforms were designed by utilizing the PET between CD composites and metal ions. For instance, Li *et al.* reported a N and S co-doped CD (N, S-CD)-based sensor for the sensitive detection of Hg^{2+} in living cells, the sensing of which was achieved through the PL quenching of N, S-CDs caused by the electron-transfer and coordination interaction between N, S-CDs and Hg^{2+} ions.[387] Following the same strategy, another group successfully accomplished the sensing of Fe^{3+} ions using a system in which N and S co-doped CDs were tagged with phenylboronic acid (N, S-CDs-PBA).[365] In this specific system, Fe^{3+} could coordinate with phenolic hydroxyl and carboxyl groups on the surface of CDs and thus excited electrons of N, S-CDs-PBA were transferred to Fe^{3+}, causing the PL quenching (Fig. 14D). Although as not frequent as PET, FRET was also a common mechanism used for detection of metal ions. For instance, in Yan and co-workers' study, glyoxylic acid-modified CDs (GA-CDs) were used as a FRET ratiometric fluorescent probe for the detection of Cu^{2+} in aqueous solution.[388] Similarly, Chen *et al.* also applied cyclam-functionalized CDs as a FRET nanoprobe for the detection of Cu^{2+} and S^{2-}.[389] In addition to the above examples, the detection of other important metal ions such as Ag^+, Cu^{2+}, Cr^{6+}, and Pb^{2+} has also been successfully realized with CD composite-based sensing platforms.[390–401]

4. Summary and outlook

In this review, recent advancements of CD-derived composites from their synthetic routes to bioapplications have been comprehensively summarized. First, we briefly introduced the properties, synthesis methods and applications of CDs. Then we carefully discussed the synthesis approaches for four types of CD composites, namely metal–CD, nonmetallic inorganics–CD, organics–CD and multi-components–CD composites. After that, the recent advancements of these CD composites for their applications in biomedical fields were also detailed. As discussed, CD composites have unique fluorescence and biological properties, rendering them suitable platforms for biomedical research, which was witnessed by the ever-increasing number of reports on this topic. Despite the above-mentioned advancements, studies on the preparation, characterization and applications of CD composites are still in their early stage, and there are several challenges that need to be addressed.

Current synthesis of CD composites generally requires two or more steps to complete, which not only demands high manufacturing cost, but also causes significant complexities in their characterization and applications. Also, the construction of CD composites is highly empirical and heavily relies on a ''trial and error'' approach! Thus, there is an urgent need to streamline the current synthesis approaches for CD composites, so that rational design of CD composites could be realized. Furthermore, most of the CD composites have not been properly isolated and purified, leaving them as mixtures of complex components with very distinct spectroscopic and biological properties after fine fractionalization. Thus, it would make sense to develop convenient and effective separation

techniques to purify the as-prepared CD composites so that samples with better uniformity could be obtained. To fulfill the potential industrial applications of CD composites, in addition to the streamlined synthesis and utilization of convenient but effective purification techniques, researchers should also focus on the development of low-cost and large-scale production of CDs. Although there have been a few reports on the large-scale (*i.e.*, kilogram-scale) preparation of CDs,[231,402] currently, the preparation of CDs on a large scale is still very hard to achieve. Recently, Xiong's group reported a novel strategy for the large-scale preparation of NIR CDs *via* a solid-state reaction, in which neither high pressure reactors nor complicated post-treatment procedures were required.[403] This safe, convenient synthesis approach might provide some inspiration for the mass production of CDs and CD composites that meet the industrial requirements.

Much effort has been devoted to the synthesis and bioapplications of CDs and CD composites; however, their biocompatibility and nano-safety issues have been of less concern. Generally speaking, carbon-based materials are inherently less toxic than metal- or semiconductor-based materials considering the intrinsic nature of carbon. Still, the cytotoxicity of CDs has raised much concern[404–406] since the toxicity of bare CDs is often dose and time dependent.[407] Surprisingly, there has been a report stating that CDs derived from the same precursors, but with different synthesis methods, demonstrated different cytotoxicities.[408] As such, researchers should devote more efforts to study and evaluate the bio-related properties of bare CDs. Regarding the biosafety of CD composites, things become more complicated since additional components (*i.e.*, metals, nonmetallic inorganics and organic molecules) are introduced, and thus these factors should be carefully reevaluated. For instance, doping with metals has been a conventional strategy to enhance the PL of CDs; however, this might reduce the biocompatibility of CDs since some of the metals might increase the toxicity of CD composites significantly. On the other hand, compositing with some materials (*i.e.*, polymers) indeed improves the biological properties of CDs; however, the enhancement of the PL performance may not be as good as that achieved by doping with metals. Thus, to obtain CD composites with superior properties for bioapplications, the types and ratios of compositing materials have to be carefully balanced! In addition, a proper evaluation method for the cytotoxicity and biocompatibility of CD composites should be carefully selected, so that the biosafety of CD composites in the context of bioapplications could be accurately and adequately assessed.

Still, we anticipate that much more effort will be devoted to CD composites and much more exciting CD composite-based applications in biomedical fields will be developed. Especially with the streamlining of the synthesis methods, introduction of effective purification techniques and accurate and adequate biosafety evaluation, CD composites with controlled compositions, tailored properties, and high biocompatibility would be feasible, which would significantly accelerate the applications of CD composites in biomedicine related fields.

Conflicts of interest

The authors declare that they have no known competing financial interests or personal relationships that could have appeared to influence the work reported in this paper.

Acknowledgements

Z. Peng gratefully acknowledges the financial support from the National Natural Science Foundation of China under the grant number: 21807010, and the Applied Basic Research Program of Yunnan Province under the grant number: 2019FB066. R. M. Leblanc gratefully acknowledges the support of the National Science Foundation under Grants 1809060 and 2041413.

References

1 S. Gogoi, S. Maji, D. Mishra, K. S. P. Devi, T. K. Maiti and N. Karak, *Macromol. Biosci.*, 2017, **17**, 1600271.
2 X. Xu and R. Ray, *J. Am. Chem. Soc.*, 2004, **126**, 12736.
3 Y.-P. Sun, B. Zhou, Y. Lin, W. Wang, K. S. Fernando, P. Pathak, M. J. Meziani, B. A. Harruff, X. Wang and H. Wang, *J. Am. Chem. Soc.*, 2006, **128**, 7756–7757.
4 S. Ganguly, P. Das, S. Banerjee and N. C. Das, *Funct. Compos. Struct.*, 2019, **1**, 022001.
5 L. Ai, Y. Yang, B. Wang, J. Chang, Z. Tang, B. Yang and S. Lu, *Sci. Bull.*, 2021, **66**, 839–856.
6 J. Yu, X. Yong, Z. Tang, B. Yang and S. Lu, *J. Phys. Chem. Lett.*, 2021, **12**, 7671–7687.
7 A. Cayuela, M. Soriano, C. Carrillo-Carrión and M. Valcárcel, *Chem. Commun.*, 2016, **52**, 1311–1326.
8 Q. Zeng, T. Feng, S. Tao, S. Zhu and B. Yang, *Light: Sci. Appl.*, 2021, **10**, 142.
9 S. Li, L. Li, H. Tu, H. Zhang, D. S. Silvester, C. E. Banks, G. Zou, H. Hou and X. Ji, *Mater. Today*, 2021, **51**, 188–207.
10 S.-L. Hu, K.-Y. Niu, J. Sun, J. Yang, N.-Q. Zhao and X.-W. Du, *J. Mater. Chem.*, 2009, **19**, 484–488.
11 Y.-P. Sun, X. Wang, F. Lu, L. Cao, M. J. Meziani, P. G. Luo, L. Gu and L. M. Veca, *J. Phys. Chem. C*, 2008, **112**, 18295–18298.
12 J. Zhou, C. Booker, R. Li, X. Zhou, T.-K. Sham, X. Sun and Z. Ding, *J. Am. Chem. Soc.*, 2007, **129**, 744–745.
13 L. Tian, D. Ghosh, W. Chen, S. Pradhan, X. Chang and S. Chen, *Chem. Mater.*, 2009, **21**, 2803–2809.
14 D. Pan, J. Zhang, Z. Li and M. Wu, *Adv. Mater.*, 2010, **22**, 734–738.
15 Y. Wang and A. Hu, *J. Mater. Chem. C*, 2014, **2**, 6921–6939.
16 H. Li, F.-Q. Shao, H. Huang, J.-J. Feng and A.-J. Wang, *Sens. Actuators, B*, 2016, **226**, 506–511.
17 L. Pan, S. Sun, A. Zhang, K. Jiang, L. Zhang, C. Dong, Q. Huang, A. Wu and H. Lin, *Adv. Mater.*, 2015, **27**, 7782–7787.
18 S. Miao, K. Liang, J. Zhu, B. Yang, D. Zhao and B. Kong, *Nano Today*, 2020, **33**, 100879.
19 Y. Ru, L. Ai, T. Jia, X. Liu, S. Lu, Z. Tang and B. Yang, *Nano Today*, 2020, **34**, 100953.

20 H. Wang, W. Su and M. Tan, *Innovation*, 2020, **1**, 100009.
21 Q. Xu, T. Kuang, Y. Liu, L. Cai, X. Peng, T. S. Sreeprasad, P. Zhao, Z. Yu and N. Li, *J. Mater. Chem. B*, 2016, **4**, 7204–7219.
22 Y. Park, J. Yoo, B. Lim, W. Kwon and S.-W. Rhee, *J. Mater. Chem. A*, 2016, **4**, 11582–11603.
23 W. Liu, C. Li, Y. Ren, X. Sun, W. Pan, Y. Li, J. Wang and W. Wang, *J. Mater. Chem. B*, 2016, **4**, 5772–5788.
24 K. Dimos, *Curr. Org. Chem.*, 2016, **20**, 682–695.
25 F. Yan, Z. Sun, H. Zhang, X. Sun, Y. Jiang and Z. Bai, *Microchim. Acta*, 2019, **186**, 583.
26 P. G. Luo, S. Sahu, S.-T. Yang, S. K. Sonkar, J. Wang, H. Wang, G. E. LeCroy, L. Cao and Y.-P. Sun, *J. Mater. Chem. B*, 2013, **1**, 2116–2127.
27 W. Wang, L. Cheng and W. Liu, *Sci. China: Chem.*, 2014, **57**, 522–539.
28 J. Pardo, Z. Peng and R. M. Leblanc, *Molecules*, 2018, **23**, 378.
29 X. Cui, L. Zhu, J. Wu, Y. Hou, P. Wang, Z. Wang and M. Yang, *Biosens. Bioelectron.*, 2015, **63**, 506–512.
30 F. Wang, S. Pang, L. Wang, Q. Li, M. Kreiter and C.-Y. Liu, *Chem. Mater.*, 2010, **22**, 4528–4530.
31 S. Anwar, H. Ding, M. Xu, X. Hu, Z. Li, J. Wang, L. Liu, L. Jiang, D. Wang, C. Dong, M. Yan, Q. Wang and H. Bi, *ACS Appl. Bio Mater.*, 2019, **2**, 2317–2338.
32 F. Yuan, S. Li, Z. Fan, X. Meng, L. Fan and S. Yang, *Nano Today*, 2016, **11**, 565–586.
33 K. Nekoueian, M. Amiri, M. Sillanpää, F. Marken, R. Boukherroub and S. Szunerits, *Chem. Soc. Rev.*, 2019, **48**, 4281–4316.
34 J. Pardo, Z. Peng and R. M. Leblanc, *Molecules*, 2018, **23**, 378.
35 H. Wu, W. Su, H. Xu, Y. Zhang, Y. Li, X. Li and L. Fan, *VIEW*, 2021, **2**, 20200061.
36 K. K. Chan, S. H. K. Yap and K.-T. Yong, *Nano-Micro Lett.*, 2018, **10**, 72.
37 H. Ding, X.-X. Zhou, J.-S. Wei, X.-B. Li, B.-T. Qin, X.-B. Chen and H.-M. Xiong, *Carbon*, 2020, **167**, 322–344.
38 D. Li, E. V. Ushakova, A. L. Rogach and S. Qu, *Small*, 2021, 2102325.
39 C. Ji, Y. Zhou, R. M. Leblanc and Z. Peng, *ACS Sens.*, 2020, **5**, 2724–2741.
40 D. Xu, Q. Lin and H.-T. Chang, *Small Methods*, 2020, **4**, 1900387.
41 B. Li, S. Zhao, L. Huang, Q. Wang, J. Xiao and M. Lan, *Chem. Eng. J.*, 2021, **408**, 127245.
42 B. Wang, H. Song, X. Qu, J. Chang, B. Yang and S. Lu, *Coord. Chem. Rev.*, 2021, **442**, 214010.
43 Z. Peng, X. Han, S. Li, A. O. Al-Youbi, A. S. Bashammakh, M. S. El-Shahawi and R. M. Leblanc, *Coord. Chem. Rev.*, 2017, **343**, 256–277.
44 Z. Peng, T. Zhao, Y. Zhou, S. Li, J. Li and R. M. Leblanc, *Adv. Healthcare Mater.*, 2020, **9**, 1901495.
45 F. Zu, F. Yan, Z. Bai, J. Xu, Y. Wang, Y. Huang and X. Zhou, *Microchim. Acta*, 2017, **184**, 1899–1914.
46 F. Li, D. Yang and H. Xu, *Chem. – Eur. J.*, 2019, **25**, 1165–1176.
47 Z. Suo, J. Dai, S. Gao and H. Gao, *Results Phys.*, 2020, 103058.
48 L. Ai, R. Shi, J. Yang, K. Zhang, T. Zhang and S. Lu, *Small*, 2021, 2007523.
49 X.-Y. Du, C.-F. Wang, G. Wu and S. Chen, *Angew. Chem., Int. Ed.*, 2021, **60**, 8585–8595.
50 L. Lin, Y. Luo, P. Tsai, J. Wang and X. Chen, *TrAC, Trends Anal. Chem.*, 2018, **103**, 87–101.
51 Y. Zhou, S. K. Sharma, Z. Peng and R. M. Leblanc, *Polymers*, 2017, **9**, 67.
52 N. Tejwan, A. K. Saini, A. Sharma, T. A. Singh, N. Kumar and J. Das, *J. Controlled Release*, 2021, **330**, 132–150.
53 A. Beiraghi and S. A. Najibi-Gehraz, *Sens. Actuators, B*, 2017, **253**, 342–351.
54 X. Zeng, Z. Wang, N. Meng, D. T. McCarthy, A. Deletic, J.-H. Pan and X. Zhang, *Appl. Catal., B*, 2017, **202**, 33–41.
55 Y. Yao, D. Niu, C. H. Lee, Y. Li and P. Li, *Macromol. Rapid Commun.*, 2019, **40**, 1800869.
56 T. Feng, X. Ai, G. An, P. Yang and Y. Zhao, *ACS Nano*, 2016, **10**, 4410–4420.
57 K. Kannan, D. Radhika, K. K. Sadasivuni, K. R. Reddy and A. V. Raghu, *Adv. Colloid Interface Sci.*, 2020, 102178.
58 J. Liu, J. Jiang, Y. Meng, A. Aihemaiti, Y. Xu, H. Xiang, Y. Gao and X. Chen, *J. Hazard. Mater.*, 2020, **388**, 122026.
59 L. Wang, Y. Li, S. Li, Y. Wang, W. Kong, W. Xue and C. Li, *J. Mater. Sci.: Mater. Electron.*, 2017, **28**, 17570–17577.
60 A. Emam, A. Mostafa, M. Mohamed, A.-S. Gadallah and M. El-Kemary, *J. Lumin.*, 2018, **200**, 287–297.
61 X. Li, Y. Fu, S. Zhao, J. Xiao, M. Lan, B. Wang, K. Zhang, X. Song and L. Zeng, *Chem. Eng. J.*, 2021, 133101, DOI: 10.1016/j.cej.2021.133101.
62 L. Wang, P. Liu, Z. Liu, H. Cao, S. Ye, K. Zhao, G. Liang and J.-J. Zhu, *Sens. Actuators, B*, 2021, **327**, 128890.
63 S. Barua, P. K. Raul, R. Gopalakrishnan, B. Das, V. Hmuaka and V. Veer, *ACS Sustainable Chem. Eng.*, 2016, **4**, 2345–2350.
64 L.-M. Shen, Q. Chen, Z.-Y. Sun, X.-W. Chen and J.-H. Wang, *Anal. Chem.*, 2014, **86**, 5002–5008.
65 Y. Zhang, B.-T. Zhang, Y. Teng, J. Zhao, L. Kuang and X. Sun, *Sep. Purif. Technol.*, 2021, **254**, 117617.
66 P.-p. Zhu, Z. Cheng, L.-l. Du, Q. Chen and K.-j. Tan, *Langmuir*, 2018, **34**, 9982–9989.
67 J. Cheng, C.-F. Wang, Y. Zhang, S. Yang and S. Chen, *RSC Adv.*, 2016, **6**, 37189–37194.
68 R. Bayan and N. Karak, *ACS Omega*, 2017, **2**, 8868–8876.
69 J. Hua, Z. Mu, P. Hua, M. Wang and K. Qin, *Talanta*, 2020, **219**, 121279.
70 J. M. Arroyave, M. E. Centurión and J. J. Prías-Barragán, *Nano-Struct. Nano-Objects*, 2020, **24**, 100596.
71 Z. Xu, H. He, S. Zhang, B. Wang, J. Jin, C. Li, X. Chen, B. Jiang and Y. Liu, *Environ. Sci.: Nano*, 2019, **6**, 1168–1179.
72 Y.-d. Cui, H. Maimaiti, S.-X. Wang, B. Xu, H.-z. Zhang and P.-s. Zhai, *NANO*, 2020, **15**, 2050103.
73 B. Das, A. Girigoswami, P. Pal and S. Dhara, *Mater. Sci. Eng., C*, 2019, **102**, 427–436.
74 S. Chen, M. Chi, Z. Yang, M. Gao, C. Wang and X. Lu, *Inorg. Chem. Front.*, 2017, **4**, 1621–1627.

75 H. Bozetine, Q. Wang, A. Barras, M. Li, T. Hadjersi, S. Szunerits and R. Boukherroub, *J. Colloid Interface Sci.*, 2016, **465**, 286–294.
76 B. De and N. Karak, *J. Mater. Chem. A*, 2017, **5**, 1826–1859.
77 Z. Guo, R. Pan, J. Cheng, L. Zhang, W. Cao and T. He, *Appl. Phys. A: Mater. Sci. Process.*, 2020, **126**, 160.
78 W. Liu, L. Tian, J. Du, J. Wu, Y. Liu, G. Wu and X. Lu, *Analyst*, 2020, **145**, 5500–5507.
79 K. Bhattacharya and P. Deb, *Dalton Trans.*, 2015, **44**, 9221–9229.
80 Q. Xu, W. Cai, M. Zhang, R. Su, Y. Ye, Y. Li, L. Zhang, Y. Guo, Z. Yu, S. Li, X. Lin, Y. Chen, Y. Luo, J. Street and M. Xu, *RSC Adv.*, 2018, **8**, 17254–17262.
81 Q. Xu, Y. Liu, R. Su, L. Cai, B. Li, Y. Zhang, L. Zhang, Y. Wang, Y. Wang and N. Li, *Nanoscale*, 2016, **8**, 17919–17927.
82 Y. Liu, J. Wei, X. Yan, M. Zhao, C. Guo and Q. Xu, *Chin. Chem. Lett.*, 2021, **32**, 861–865.
83 W. Qing, K. Chen, Y. Yang, Y. Wang and X. Liu, *Microchem. J.*, 2020, **152**, 104262.
84 M. Zhang, W. Wang, P. Yuan, C. Chi, J. Zhang and N. Zhou, *Chem. Eng. J.*, 2017, **330**, 1137–1147.
85 H. Yu, Y. Zhao, C. Zhou, L. Shang, Y. Peng, Y. Cao, L.-Z. Wu, C.-H. Tung and T. Zhang, *J. Mater. Chem. A*, 2014, **2**, 3344–3351.
86 Y. Zhu, Z. Wu, M. Jing, H. Hou, Y. Yang, Y. Zhang, X. Yang, W. Song, X. Jia and X. Ji, *J. Mater. Chem. A*, 2015, **3**, 866–877.
87 Z. Zeng, F.-X. Xiao, H. Phan, S. Chen, Z. Yu, R. Wang, T.-Q. Nguyen and T. T. Y. Tan, *J. Mater. Chem. A*, 2018, **6**, 1700–1713.
88 Y. Yang, C. Zhang, D. Huang, G. Zeng, J. Huang, C. Lai, C. Zhou, W. Wang, H. Guo and W. Xue, *Appl. Catal., B*, 2019, **245**, 87–99.
89 Y. Wang, L. Mao, W. Liu, F. Ding, P. Zou, X. Wang, Q. Zhao and H. Rao, *Microchim. Acta*, 2018, **185**, 442.
90 B. Wu, Y. Kuang, X. Zhang and J. Chen, *Nano Today*, 2011, **6**, 75–90.
91 Y. Liu, Y. Zhao, Q. Fan, M. S. Khan, X. Li, Y. Zhang, H. Ma and Q. Wei, *Microchim. Acta*, 2018, **185**, 85.
92 Y. Fu, G. Zeng, C. Lai, D. Huang, L. Qin, H. Yi, X. Liu, M. Zhang, B. Li and S. Liu, *Chem. Eng. J.*, 2020, 125743.
93 Q. Huang, H. Zhang, S. Hu, F. Li, W. Weng, J. Chen, Q. Wang, Y. He, W. Zhang and X. Bao, *Biosens. Bioelectron.*, 2014, **52**, 277–280.
94 H. Ge, K. Zhang, H. Yu, J. Yue, L. Yu, X. Chen, T. Hou, K. A. Alamry, H. M. Marwani and S. Wang, *J. Fluoresc.*, 2018, **28**, 1405–1412.
95 H. Zheng, Q. Wang, Y. Long, H. Zhang, X. Huang and R. Zhu, *Chem. Commun.*, 2011, **47**, 10650–10652.
96 X. Wang, Y. Long, Q. Wang, H. Zhang, X. Huang, R. Zhu, P. Teng, L. Liang and H. Zheng, *Carbon*, 2013, **64**, 499–506.
97 S. Mandani, B. Sharma, D. Dey and T. K. Sarma, *Nanoscale*, 2015, **7**, 1802–1808.
98 P. Luo, C. Li and G. Shi, *Phys. Chem. Chem. Phys.*, 2012, **14**, 7360–7366.
99 J. Xu, S. Sahu, L. Cao, C. E. Bunker, G. Peng, Y. Liu, K. A. S. Fernando, P. Wang, E. A. Guliants, M. J. Meziani, H. Qian and Y.-P. Sun, *Langmuir*, 2012, **28**, 16141–16147.
100 Q. Huang, X. Lin, J.-J. Zhu and Q.-X. Tong, *Biosens. Bioelectron.*, 2017, **94**, 507–512.
101 S. Han, H. Zhang, Y. Xie, L. Liu, C. Shan, X. Li, W. Liu and Y. Tang, *Appl. Surf. Sci.*, 2015, **328**, 368–373.
102 S. A. Rub Pakkath, S. S. Chetty, P. Selvarasu, A. Vadivel Murugan, Y. Kumar, L. Periyasamy, M. Santhakumar, S. R. Sadras and K. Santhakumar, *ACS Biomater. Sci. Eng.*, 2018, **4**, 2582–2596.
103 V. B. Kumar, R. Kumar, A. Gedanken and O. Shefi, *Ultrason. Sonochem.*, 2019, **52**, 205–213.
104 M. Li Liu, B. B. Chen, T. Yang, J. Wang, X. Dong Liu and C. Zhi Huang, *Methods Appl. Fluoresc.*, 2017, **5**, 015003.
105 L. Wu, M. Li, M. Zhang, M. Yan, S. Ge and J. Yu, *Sens. Actuators, B*, 2013, **186**, 761–767.
106 Y. Dong, J. Zhang, P. Jiang, G. Wang, X. Wu, H. Zhao and C. Zhang, *New J. Chem.*, 2015, **39**, 4141–4146.
107 S. Lee, G. Baek, J.-H. Lee, D.-W. Choi, B. Shong and J.-S. Park, *Appl. Surf. Sci.*, 2018, **458**, 864–871.
108 X. Zhang, Z. Sun, Z. Zhu, J. Luo, Z. Wu and Z. Wang, Ceram. Int., 2020.
109 M. Amjadi and R. Jalili, *Biosens. Bioelectron.*, 2017, **96**, 121–126.
110 Q. Li, H. Cheng, X. Wu, C.-F. Wang, G. Wu and S. Chen, *J. Mater. Chem. A*, 2018, **6**, 14112–14119.
111 N. Lim, J.-S. Lee and Y. T. Byun, *Nanomaterials*, 2020, **10**, 2509.
112 J. Pan, Y. Sheng, J. Zhang, J. Wei, P. Huang, X. Zhang and B. Feng, *J. Mater. Chem. A*, 2014, **2**, 18082–18086.
113 F. Li, D. Yang and H. Xu, *Chem. – Eur. J.*, 2019, **25**, 1165–1176.
114 Q. Xu, T. Kuang, Y. Liu, L. Cai, X. Peng, T. Sreenivasan Sreeprasad, P. Zhao, Z. Yu and N. Li, *J. Mater. Chem. B*, 2016, **4**, 7204–7219.
115 C. Bie, B. Zhu, F. Xu, L. Zhang and J. Yu, *Adv. Mater.*, 2019, **31**, 1902868.
116 N. A. Travlou, J. Secor and T. J. Bandosz, *Carbon*, 2017, **114**, 544–556.
117 Y. Ma, A. Chen, Y. Huang, X. He, X. Xie, B. He, J. Yang and X. Wang, *Carbon*, 2020, **162**, 234–244.
118 C. V. Raju, G. Kalaiyarasan, S. Paramasivam, J. Joseph and S. S. Kumar, *Electrochim. Acta*, 2020, **331**, 135391.
119 M. Amjadi, T. Hallaj, J. L. Manzoori and T. Shahbazsaghir, *Spectrochim. Acta, Part A*, 2018, **201**, 223–228.
120 Z. Qian, X. Shan, L. Chai, J. Ma, J. Chen and H. Feng, *ACS Appl. Mater. Interfaces*, 2014, **6**, 6797–6805.
121 P. Long, Y. Feng, C. Cao, Y. Li, J. Han, S. Li, C. Peng, Z. Li and W. Feng, *Adv. Funct. Mater.*, 2018, **28**, 1800791.
122 J. Zhang, D. Nan, S. Pan, H. Liu, H. Yang and X. Hu, *Spectrochim. Acta, Part A*, 2019, **221**, 117161.
123 A. Pathak, P. Suneesh, J. Stanley and T. S. Babu, *Microchim. Acta*, 2019, **186**, 157.
124 T. Chatzimitakos, A. Kasouni, L. Sygellou, I. Leonardos, A. Troganis and C. Stalikas, *Sens. Actuators, B*, 2018, **267**, 494–501.

125 R. Anjana, J. A. Devi, M. Jayasree, R. Aparna, B. Aswathy, G. Praveen, G. Lekha and G. Sony, *Microchim. Acta*, 2018, **185**, 11.
126 Y. Tu, S. Wang, X. Yuan, Y. Wei, K. Qin, Q. Zhang, X. Chen and X. Ji, *Dyes Pigm.*, 2020, 108316.
127 W. K. Kipnusu, C. Doñate-Buendía, M. Fernández-Alonso, J. Lancis and G. Mínguez-Vega, *Part. Part. Syst. Charact.*, 2020, 2000093.
128 T. Tian, Y. He, Y. Ge and G. Song, *Sens. Actuators, B*, 2017, **240**, 1265–1271.
129 S. Huang, E. Yang, J. Yao, Y. Liu and Q. Xiao, *Anal. Chim. Acta*, 2018, **1035**, 192–202.
130 S. Song, J. Hu, M. Li, X. Gong, C. Dong and S. Shuang, *Mater. Sci. Eng., C*, 2021, **118**, 111478.
131 W. Dong, R. Wang, X. Gong, W. Liang, L. Fan, S. Song and C. Dong, *Microchim. Acta*, 2020, **187**, 1–12.
132 Y. Yan, Q. Huang, C. Wei, S. Hu, H. Zhang, W. Zhang, W. Yang, P. Dong, M. Zhu and Z. Wang, *RSC Adv.*, 2016, **6**, 115317–115325.
133 H. Yang, J. Hong, L. Wei and C. Deng, *Ceram. Int.*, 2018, **44**, 16844–16850.
134 H. Li, X. Wang, Z. Cai, L. Lu, J. Tao, B. Sun, Y. Yang, Q. Xu, Z. Yu and P. Zhao, *Anal. Bioanal. Chem.*, 2017, **409**, 6655–6662.
135 X. Li, H. Lin, Q. Li, J. Xue, Y. Xu and L. Zhuang, *ACS Appl. Nano Mater.*, 2021, **4**, 3062–3074.
136 Y. Ye, D. Zhang, Y. Zou, H. Zhao and H. Chen, *J. Cleaner Prod.*, 2020, 121682.
137 Y. Wu, Y. Liu, J. Yin, H. Li and J. Huang, *Talanta*, 2019, **205**, 120121.
138 L. L. Pérez, S. Perdriau, G. T. Brink, B. J. Kooi, H. J. Heeres and I. Melián-Cabrera, *Chem. Mater.*, 2013, **25**, 848–855.
139 T. Bala, G. Armstrong, F. Laffir and R. Thornton, *J. Colloid Interface Sci.*, 2011, **356**, 395–403.
140 B. G. Fouda-Mbanga, E. Prabakaran and K. Pillay, *Arabian J. Chem.*, 2020, **13**, 6762–6781.
141 Y. He, J. He, L. Wang, Z. Yu, H. Zhang, Y. Liu and B. Lei, *Sens. Actuators, B*, 2017, **251**, 918–926.
142 Y. He, J. He, H. Zhang, Y. Liu and B. Lei, *J. Colloid Interface Sci.*, 2017, **496**, 8–15.
143 Y. Wang, C. Zhang, X. Chen, B. Yang, L. Yang, C. Jiang and Z. Zhang, *Nanoscale*, 2016, **8**, 5977–5984.
144 W. Wang, E. Eftekhari, G. Zhu, X. Zhang, Z. Yan and Q. Li, *Chem. Commun.*, 2014, **50**, 13089–13092.
145 H. Zhu, W. Zhang, K. Zhang and S. Wang, *Nanotechnology*, 2012, **23**, 315502.
146 Y. Ding, S. Z. Shen, H. Sun, K. Sun and F. Liu, *Sens. Actuators, B*, 2014, **203**, 35–43.
147 Z. Liu, S. Liu, P. Yin and Y. He, *Anal. Chim. Acta*, 2012, **745**, 78–84.
148 B. Cao, C. Yuan, B. Liu, C. Jiang, G. Guan and M.-Y. Han, *Anal. Chim. Acta*, 2013, **786**, 146–152.
149 J. Bai, C. Sun and X. Jiang, *Anal. Bioanal. Chem.*, 2016, **408**, 4705–4714.
150 B. RasulKhan, P. Periakaruppan, S. K. Ponnaiah, G. Venkatachalam and B. Jeyaprabha, *J. Cluster Sci.*, 2021, **32**, 135–144.
151 W. Li, S. Wu, X. Xu, J. Zhuang, H. Zhang, X. Zhang, C. Hu, B. Lei, C. F. Kaminski and Y. Liu, *Chem. Mater.*, 2019, **31**, 9887–9894.
152 W. Suchanek and M. Yoshimura, *J. Mater. Res.*, 1998, **13**, 94–117.
153 Z. Peng, T. Zhao, Y. Zhou, S. Li, J. Li and R. M. Leblanc, *Adv. Healthcare Mater.*, 2020, **9**, 1901495.
154 F. C. Fierz, F. Beckmann, M. Huser, S. H. Irsen, B. Leukers, F. Witte, Ö. Degistirici, A. Andronache, M. Thie and B. Müller, *Biomaterials*, 2008, **29**, 3799–3806.
155 H. K. Chung, V. Wongso, N. S. Sambudi and I. Isnaeni, *J. Sol-Gel Sci. Technol.*, 2020, **93**, 214–223.
156 M. Irfan, A. Jeshurun, P. Baraneedharan and B. M. Reddy, *Mater. Technol.*, 2021, 1–12, DOI: 10.1080/10667857.2021.1879529.
157 D. Jiang, H. Zhao, Y. Yang, Y. Zhu, X. Chen, J. Sun, K. Yu, H. Fan and X. Zhang, *J. Mater. Chem. B*, 2017, **5**, 3749–3757.
158 S. Gogoi, M. Kumar, B. B. Mandal and N. Karak, *RSC Adv.*, 2016, **6**, 26066–26076.
159 D. K. Khajuria, V. B. Kumar, D. Gigi, A. Gedanken and D. Karasik, *ACS Appl. Mater. Interfaces*, 2018, **10**, 19373–19385.
160 Q. Chang, K. K. Li, S. L. Hu, Y. G. Dong and J. L. Yang, *Mater. Lett.*, 2016, **175**, 44–47.
161 R. Jalili and M. Amjadi, *RSC Adv.*, 2015, **5**, 74084–74090.
162 P.-C. Chen, Y.-N. Chen, P.-C. Hsu, C.-C. Shih and H.-T. Chang, *Chem. Commun.*, 2013, **49**, 1639–1641.
163 A. K. Geim, *Science*, 2009, **324**, 1530–1534.
164 K. Zhou, Y. Zhu, X. Yang, J. Luo, C. Li and S. Luan, *Electrochim. Acta*, 2010, **55**, 3055–3060.
165 X. Geng, L. Niu, Z. Xing, R. Song, G. Liu, M. Sun, G. Cheng, H. Zhong, Z. Liu, Z. Zhang, L. Sun, H. Xu, L. Lu and L. Liu, *Adv. Mater.*, 2010, **22**, 638–642.
166 C.-I. Wang, A. P. Periasamy and H.-T. Chang, *Anal. Chem.*, 2013, **85**, 3263–3270.
167 S. Hu, Q. Huang, Y. Lin, C. Wei, H. Zhang, W. Zhang, Z. Guo, X. Bao, J. Shi and A. Hao, *Electrochim. Acta*, 2014, **130**, 805–809.
168 J. Shin, J. Guo, T. Zhao and Z. Guo, *Small*, 2019, **15**, 1900296.
169 C. Hu, C. Yu, M. Li, X. Wang, Q. Dong, G. Wang and J. Qiu, *Chem. Commun.*, 2015, **51**, 3419–3422.
170 X. Yang, L. Sui, B. Wang, Y. Zhang, Z. Tang, B. Yang and S. Lu, *Sci. China: Chem.*, 2021, 64, 1547–1553.
171 X. Liu, X. Hu, Z. Xie, P. Chen, X. Sun, J. Yan and S. Zhou, *Anal. Methods*, 2016, **8**, 3236–3241.
172 Q. Chang, X. Meng, S. L. Hu, F. Zhang and J. L. Yang, *RSC Adv.*, 2017, **7**, 30191–30198.
173 M. Massaro, C. G. Colletti, S. Guernelli, G. Lazzara, M. Liu, G. Nicotra, R. Noto, F. Parisi, I. Pibiri, C. Spinella and S. Riela, *J. Mater. Chem. C*, 2018, **6**, 7377–7384.
174 M. Ali, R. Riaz, A. S. Anjum, K. C. Sun, H. Li, S. Ahn, S. H. Jeong and M. J. Ko, *J. Colloid Interface Sci.*, 2021, **586**, 349–361.
175 Z. Shen, C. Zhang, X. Yu, J. Li, Z. Wang, Z. Zhang and B. Liu, *J. Mater. Chem. C*, 2018, **6**, 9636–9641.

176 X. Song, Q. Guo, Z. Cai, J. Qiu and G. Dong, *Ceram. Int.*, 2019, **45**, 17387–17394.
177 C.-C. Shih, P.-C. Chen, G.-L. Lin, C.-W. Wang and H.-T. Chang, *ACS Nano*, 2015, **9**, 312–319.
178 Y.-B. Zhao, Y.-j. Ma, D. Song, Y. Liu, Y. Luo, S. Lin and C.-y. Liu, *Anal. Methods*, 2017, **9**, 4770–4775.
179 A. Konwar, N. Gogoi, G. Majumdar and D. Chowdhury, *Carbohydr. Polym.*, 2015, **115**, 238–245.
180 X. Li, S. Zhang, S. A. Kulinich, Y. Liu and H. Zeng, *Sci. Rep.*, 2014, **4**, 4976.
181 B. Han, W. Wang, H. Wu, F. Fang, N. Wang, X. Zhang and S. Xu, *Colloids Surf., B*, 2012, **100**, 209–214.
182 Z. Yuan, X. Wu, Y. Jiang, Y. Li, J. Huang, L. Hao, J. Zhang and J. Wang, *J. Membr. Sci.*, 2018, **549**, 1–11.
183 Y. Liu, P. Wang, K. S. Fernando, G. E. LeCroy, H. Maimaiti, B. A. Harruff-Miller, W. K. Lewis, C. E. Bunker, Z.-L. Hou and Y.-P. Sun, *J. Mater. Chem. C*, 2016, **4**, 6967–6974.
184 F. Wu, L. Yue, H. Su, K. Wang, L. Yang and X. Zhu, *Nanoscale Res. Lett.*, 2018, **13**, 357.
185 J. Zhang, M. Zheng, F. Zhang, B. Xu, W. Tian and Z. Xie, *Chem. Mater.*, 2016, **28**, 8825–8833.
186 L. Wei, Y. Ma, X. Shi, Y. Wang, X. Su, C. Yu, S. Xiang, L. Xiao and B. Chen, *J. Mater. Chem. B*, 2017, **5**, 3383–3390.
187 X. Zhao, J. Zhang, L. Shi, M. Xian, C. Dong and S. Shuang, *RSC Adv.*, 2017, **7**, 42159–42167.
188 Y. Song, Y. Chen, L. Feng, J. Ren and X. Qu, *Chem. Commun.*, 2011, **47**, 4436–4438.
189 A. Sachdev, I. Matai, S. U. Kumar, B. Bhushan, P. Dubey and P. Gopinath, *RSC Adv.*, 2013, **3**, 16958–16961.
190 N. Arsalani, P. Nezhad-Mokhtari and E. Jabbari, *Artif. Cells, Nanomed., Biotechnol.*, 2019, **47**, 540–547.
191 B.-X. Zhang, G.-Y. Zhang, H. Gao, S.-H. Wu, J.-H. Chen and X.-L. Li, *RSC Adv.*, 2015, **5**, 7395–7400.
192 Z. Peng, C. Ji, Y. Zhou, T. Zhao and R. M. Leblanc, *Appl. Mater. Today*, 2020, **20**, 100677.
193 C.-C. Fu, C.-Y. Wu, C.-C. Chien, T.-H. Hsu, S.-F. Ou, S.-T. Chen, C.-H. Wu, C.-T. Hsieh, R.-S. Juang and Y.-H. Hsueh, *Nanomaterials*, 2020, **10**, 677.
194 A. Sachdev, I. Matai and P. Gopinath, *RSC Adv.*, 2014, **4**, 20915–20921.
195 Y. Dong, R. Wang, H. Li, J. Shao, Y. Chi, X. Lin and G. Chen, *Carbon*, 2012, **50**, 2810–2815.
196 H. Zeng, L. Li, Y. Ding and Q. Zhuang, *Talanta*, 2018, **178**, 879–885.
197 J. J. Huang, Z. F. Zhong, M. Z. Rong, X. Zhou, X. D. Chen and M. Q. Zhang, *Carbon*, 2014, **70**, 190–198.
198 M. C. Kim, K. S. Yu, S. Y. Han, J.-J. Kim, J. W. Lee, N. S. Lee, Y. G. Jeong and D. K. Kim, *Eur. Polym. J.*, 2018, **98**, 191–198.
199 I. Martins, H. Tomás, F. Lahoz and J. Rodrigues, *Biomacromolecules*, 2021, **22**, 2436–2450.
200 Z. Zhu, Z. Sun, Z. Guo, X. Zhang and Z.-C. Wu, *J. Colloid Interface Sci.*, 2019, **552**, 572–582.
201 S. Lu, L. Sui, J. Liu, S. Zhu, A. Chen, M. Jin and B. Yang, *Adv. Mater.*, 2017, **29**, 1603443.
202 B. Wang, J. Li, Z. Tang, B. Yang and S. Lu, *Sci. Bull.*, 2019, **64**, 1285–1292.
203 L. Li, D. Liu, H. Mao and T. You, *Biosens. Bioelectron.*, 2017, **89**, 489–495.
204 C. Liu, P. Zhang, X. Zhai, F. Tian, W. Li, J. Yang, Y. Liu, H. Wang, W. Wang and W. Liu, *Biomaterials*, 2012, **33**, 3604–3613.
205 J.-Y. Yin, H.-J. Liu, S. Jiang, Y. Chen and Y. Yao, *ACS Macro Lett.*, 2013, **2**, 1033–1037.
206 H. Liu, Q. Wang, G. Shen, C. Zhang, C. Li, W. Ji, C. Wang and D. Cui, *Nanoscale Res. Lett.*, 2014, **9**, 397.
207 L. Li, T. Zhang, J. Lü and C. Lü, *Appl. Surf. Sci.*, 2018, **454**, 181–191.
208 X. Zhao, W. Shen, Q. Dang, F. Liao, W. Zhu, H. Shi and M. Shao, *J. Appl. Electrochem.*, 2020, **50**, 925–933.
209 D.-Q. Feng, G. Liu, Z. Chen, H. Lu, Y. Gao and X. Fang, *Microchem. J.*, 2020, **157**, 104977.
210 F. Li, C. Liu, J. Yang, Z. Wang, W. Liu and F. Tian, *RSC Adv.*, 2014, **4**, 3201–3205.
211 H. Lv, Y. Yuan, Q. Xu, H. Liu, Y.-G. Wang and Y. Xia, *J. Power Sources*, 2018, **398**, 167–174.
212 Y. Zhou and Z. Ma, *Sens. Actuators, B*, 2016, **233**, 426–430.
213 S. Asadzadeh-Khaneghah, A. Habibi-Yangjeh, D. Seifzadeh, H. Chand and V. Krishnan, *Adv. Powder Technol.*, 2021, **32**, 1196–1206.
214 M. Ganesan, K. D. Ramadhass, H.-C. Chuang and G. Gopalakrishnan, *J. Mol. Liq.*, 2021, **331**, 115768.
215 Y. Liu, C.-Y. Liu, Z.-Y. Zhang, W.-D. Yang and S.-D. Nie, *J. Mater. Chem. C*, 2015, **3**, 2881–2885.
216 H. Sun, L. Wu, W. Wei and X. Qu, *Mater. Today*, 2013, **16**, 433–442.
217 A. Meng, Q. Xu, K. Zhao, Z. Li, J. Liang and Q. Li, *Sens. Actuators, B*, 2018, **255**, 657–665.
218 Z. Qian, J. Ma, X. Shan, H. Feng, L. Shao and J. Chen, *Chem. – Eur. J.*, 2014, **20**, 2254–2263.
219 Y. Liu, P. Wu, X. Wu, C. Ma, S. Luo, M. Xu, W. Li and S. Liu, *Talanta*, 2020, **210**, 120649.
220 T. Liu, N. Li, J. X. Dong, H. Q. Luo and N. B. Li, *Sens. Actuators, B*, 2016, **231**, 147–153.
221 S. Jayaweera, K. Yin, X. Hu and W. J. Ng, *J. Fluoresc.*, 2019, **29**, 1291–1300.
222 L. S. Walekar, P. Hu, F. Liao, X. Guo and M. Long, *Microchim. Acta*, 2018, **185**, 31.
223 W.-S. Zou, W.-L. Kong, Q.-C. Zhao, J. Zhang, X. Zhao, D. Zhao and Y.-Q. Wang, *Microchim. Acta*, 2019, **186**, 576.
224 D. Bano, S. Chandra, P. K. Yadav, V. K. Singh and S. H. Hasan, *J. Photochem. Photobiol., A*, 2020, 112558.
225 S. K. Tammina, Y. Wan, Y. Li and Y. Yang, *J. Photochem. Photobiol., B*, 2020, **202**, 111734.
226 M. Li, M. Wang, L. Zhu, Y. Li, Z. Yan, Z. Shen and X. Cao, *Appl. Catal., B*, 2018, **231**, 269–276.
227 P. R. Sreenath, S. Mandal, S. Singh, H. Panigrahi, P. Das, A. K. Bhowmick and K. Dinesh Kumar, *Eur. Polym. J.*, 2020, **123**, 109454.
228 J. Deng, Q. Lu, Y. Hou, M. Liu, H. Li, Y. Zhang and S. Yao, *Anal. Chem.*, 2015, **87**, 2195–2203.
229 G. Hong, A. L. Antaris and H. Dai, *Nat. Biomed. Eng.*, 2017, **1**, 0010.

230 R. Weissleder, *Nat. Biotechnol.*, 2001, **19**, 316–317.
231 W. Li, Y. Liu, B. Wang, H. Song, Z. Liu, S. Lu and B. Yang, *Chin. Chem. Lett.*, 2019, **30**, 2323–2327.
232 H. Ali, S. Ghosh and N. R. Jana, *Wiley Interdiscip. Rev.: Nanomed. Nanobiotechnol.*, 2020, **12**, e1617.
233 Z. Xu, J. Liu, K. Wang, B. Yan, S. Hu, X. Ren and Z. Gao, *Environ. Sci. Pollut. Res.*, 2021, **28**(16), 19878–19889.
234 Z. Yi, X. Li, H. Zhang, X. Ji, W. Sun, Y. Yu, Y. Liu, J. Huang, Z. Sarshar and M. Sain, *Talanta*, 2021, **222**, 121663.
235 J. Jia, W. Lu, L. Li, Y. Gao, Y. Jiao, H. Han, C. Dong and S. Shuang, *J. Mater. Chem. B*, 2020, **8**, 2123–2127.
236 X. Gong, W. Lu, M. C. Paau, Q. Hu, X. Wu, S. Shuang, C. Dong and M. M. Choi, *Anal. Chim. Acta*, 2015, **861**, 74–84.
237 H. Wang, J. Di, Y. Sun, J. Fu, Z. Wei, H. Matsui, A. D. C. Alonso and S. Zhou, *Adv. Funct. Mater.*, 2015, **25**, 5537–5547.
238 S. Huang, E. Yang, Y. Liu, J. Yao, W. Su and Q. Xiao, *Sens. Actuators, B*, 2018, **265**, 326–334.
239 P. Ni, Q. Li, C. Xu, H. Lai, Y. Bai and T. Chen, *Appl. Surf. Sci.*, 2019, **494**, 377–383.
240 L. Yang, W. Jiang, L. Qiu, X. Jiang, D. Zuo, D. Wang and L. Yang, *Nanoscale*, 2015, **7**, 6104–6113.
241 L. Wu, X. Li, Y. Ling, C. Huang and N. Jia, *ACS Appl. Mater. Interfaces*, 2017, **9**, 28222–28232.
242 Y. Rong, C. Wu, J. Yu, X. Zhang, F. Ye, M. Zeigler, M. E. Gallina, I. C. Wu, Y. Zhang, Y.-H. Chan, W. Sun, K. Uvdal and D. T. Chiu, *ACS Nano*, 2013, **7**, 376–384.
243 V. Borse, M. Thakur, S. Sengupta and R. Srivastava, *Sens. Actuators, B*, 2017, **248**, 481–492.
244 R. Atchudan, T. N. J. I. Edison, K. R. Aseer, S. Perumal and Y. R. Lee, *Colloids Surf., B*, 2018, **169**, 321–328.
245 C. Cheng, M. Xing and Q. Wu, *Opt. Mater.*, 2019, **88**, 353–358.
246 D. Qu, X. Miao, X. Wang, C. Nie, Y. Li, L. Luo and Z. Sun, *J. Mater. Chem. B*, 2017, **5**, 4988–4992.
247 L. Zhang, D. Wang, H. Huang, L. Liu, Y. Zhou, X. Xia, K. Deng and X. Liu, *ACS Appl. Mater. Interfaces*, 2016, **8**, 6646–6655.
248 D. J. Bharali, D. W. Lucey, H. Jayakumar, H. E. Pudavar and P. N. Prasad, *J. Am. Chem. Soc.*, 2005, **127**, 11364–11371.
249 N. Parker, M. J. Turk, E. Westrick, J. D. Lewis, P. S. Low and C. P. Leamon, *Anal. Biochem.*, 2005, **338**, 284–293.
250 A. Nasrin, M. Hassan and V. G. Gomes, *Nanoscale*, 2020, **12**, 20598–20603.
251 S. Ruan, J. Qian, S. Shen, J. Zhu, X. Jiang, Q. He and H. Gao, *Nanoscale*, 2014, **6**, 10040–10047.
252 X. Wen, Z. Zhao, S. Zhai, X. Wang and Y. Li, *Diamond Relat. Mater.*, 2020, **105**, 107791.
253 X. Bao, Y. Yuan, J. Chen, B. Zhang, D. Li, D. Zhou, P. Jing, G. Xu, Y. Wang, K. Holá, D. Shen, C. Wu, L. Song, C. Liu, R. Zbořil and S. Qu, *Light: Sci. Appl.*, 2018, **7**, 91.
254 B. B. Karakoçak, J. Liang, S. Kavadiya, M. Y. Berezin, P. Biswas and N. Ravi, *ACS Appl. Nano Mater.*, 2018, **1**, 3682–3692.
255 F. Cui, J. Sun, J. de Dieu Habimana, X. Yang, J. Ji, Y. Zhang, H. Lei, Z. Li, J. Zheng, M. Fan and X. Sun, *Anal. Chem.*, 2019, **91**, 14681–14690.
256 R. Atchudan, T. N. J. I. Edison, S. Perumal, N. Clament Sagaya Selvam and Y. R. Lee, *J. Photochem. Photobiol., A*, 2019, **372**, 99–107.
257 T. Pal, S. Mohiyuddin and G. Packirisamy, *ACS Omega*, 2018, **3**, 831–843.
258 M. Zhang, T. Zheng, B. Sheng, F. Wu, Q. Zhang, W. Wang, J. Shen, N. Zhou and Y. Sun, *Chem. Eng. J.*, 2019, **373**, 1054–1063.
259 L. V. Wang and S. Hu, *Science*, 2012, **335**, 1458–1462.
260 C. Lee, W. Kwon, S. Beack, D. Lee, Y. Park, H. Kim, S. K. Hahn, S.-W. Rhee and C. Kim, *Theranostics*, 2016, **6**, 2196–2208.
261 Q. Jia, J. Ge, W. Liu, S. Liu, G. Niu, L. Guo, H. Zhang and P. Wang, *Nanoscale*, 2016, **8**, 13067–13077.
262 N. Parvin and T. K. Mandal, *Microchim. Acta*, 2017, **184**, 1117–1125.
263 D. Ni, W. Bu, E. B. Ehlerding, W. Cai and J. Shi, *Chem. Soc. Rev.*, 2017, **46**, 7438–7468.
264 R. Di Corato, F. Gazeau, C. Le Visage, D. Fayol, P. Levitz, F. Lux, D. Letourneur, N. Luciani, O. Tillement and C. Wilhelm, *ACS Nano*, 2013, **7**, 7500–7512.
265 J. Aakash, R. Choubey, D. Das and S. Mukherjee, *J. Alloys Compd.*, 2016, **668**, 33–39.
266 W. A. High, R. A. Ayers, J. Chandler, G. Zito and S. E. Cowper, *J. Am. Acad. Dermatol.*, 2007, **56**, 21–26.
267 H. Wang, X. Na, S. Liu, H. Liu, L. Zhang, M. Xie, Z. Jiang, F. Han, Y. Li, S. Cheng and M. Tan, *Talanta*, 2019, **201**, 388–396.
268 N. Nimi, A. Saraswathy, S. S. Nazeer, N. Francis, S. J. Shenoy and R. S. Jayasree, *Biomaterials*, 2018, **171**, 46–56.
269 S. Sun, L. Zhao, D. Wu, H. Zhang, H. Lian, X. Zhao, A. Wu and L. Zeng, *ACS Appl. Bio Mater.*, 2021, **4**(2), 1969–1975.
270 F. Du, L. Zhang, L. Zhang, M. Zhang, A. Gong, Y. Tan, J. Miao, Y. Gong, M. Sun, H. Ju, C. Wu and S. Zou, *Biomaterials*, 2017, **121**, 109–120.
271 Y. Wang, T. Wang, X. Chen, Y. Xu and H. Li, *Opt. Mater.*, 2018, **78**, 118–125.
272 A. B. Bourlinos, A. Bakandritsos, A. Kouloumpis, D. Gournis, M. Krysmann, E. P. Giannelis, K. Polakova, K. Safarova, K. Hola and R. Zboril, *J. Mater. Chem.*, 2012, **22**, 23327–23330.
273 H. Liao, Z. Wang, S. Chen, H. Wu, X. Ma and M. Tan, *RSC Adv.*, 2015, **5**, 66575–66581.
274 Y. Wu, H. Li, Y. Yan, K. Wang, Y. Cheng, Y. Li, X. Zhu, J. Xie and X. Sun, *Int. J. Nanomed.*, 2020, **15**, 4691.
275 Y. Zhao, X. Hao, W. Lu, R. Wang, X. Shan, Q. Chen, G. Sun and J. Liu, *ACS Appl. Nano Mater.*, 2018, **1**, 2544–2551.
276 F. Arcamone, G. Franceschi, S. Penco and A. Selva, *Tetrahedron Lett.*, 1969, **10**, 1007–1010.
277 H. Gao, A. V. Sapelkin, M. M. Titirici and G. B. Sukhorukov, *ACS Nano*, 2016, **10**, 9608–9615.
278 T. Feng, X. Ai, H. Ong and Y. Zhao, *ACS Appl. Mater. Interfaces*, 2016, **8**, 18732–18740.
279 P. Gong, J. Du, D. Wang, B. Cao, M. Tian, Y. Wang, L. Sun, S. Ji and Z. Liu, *J. Mater. Chem. B*, 2018, **6**, 2769–2777.

280 T. Yang, J.-L. Huang, Y.-T. Wang, A.-Q. Zheng, Y. Shu and J.-H. Wang, *ChemNanoMat*, 2019, **5**, 479–487.
281 Q. Wang, X. Huang, Y. Long, X. Wang, H. Zhang, R. Zhu, L. Liang, P. Teng and H. Zheng, *Carbon*, 2013, **59**, 192–199.
282 P. Gong, S. Ji, J. Wang, D. Dai, F. Wang, M. Tian, L. Zhang, F. Guo and Z. Liu, *Chem. Eng. J.*, 2018, **348**, 438–446.
283 M. Zhang, P. Yuan, N. Zhou, Y. Su, M. Shao and C. Chi, *RSC Adv.*, 2017, **7**, 9347–9356.
284 P. Gong, L. Sun, F. Wang, X. Liu, Z. Yan, M. Wang, L. Zhang, Z. Tian, Z. Liu and J. You, *Chem. Eng. J.*, 2019, **356**, 994–1002.
285 X. He, Q. Luo, J. Zhang, P. Chen, H.-J. Wang, K. Luo and X.-Q. Yu, *Nanoscale*, 2019, **11**, 12973–12982.
286 X.-Y. Zheng, K. Zhao, J. Tang, X.-Y. Wang, L.-D. Li, N.-X. Chen, Y.-J. Wang, S. Shi, X. Zhang, S. Malaisamy, L.-D. Sun, X. Wang, C. Chen and C.-H. Yan, *ACS Nano*, 2017, **11**, 3642–3650.
287 C.-W. Lai, Y.-H. Hsiao, Y.-K. Peng and P.-T. Chou, *J. Mater. Chem.*, 2012, **22**, 14403–14409.
288 N. Gao, W. Yang, H. Nie, Y. Gong, J. Jing, L. Gao and X. Zhang, *Biosens. Bioelectron.*, 2017, **96**, 300–307.
289 X. Wang, X. Li, Y. Mao, D. Wang, Q. Zhao and S. Wang, *J. Colloid Interface Sci.*, 2019, **552**, 639–650.
290 S. Pandey, M. Thakur, A. Mewada, D. Anjarlekar, N. Mishra and M. Sharon, *J. Mater. Chem. B*, 2013, **1**, 4972–4982.
291 Y.-Y. Yao, G. Gedda, W. M. Girma, C.-L. Yen, Y.-C. Ling and J.-Y. Chang, *ACS Appl. Mater. Interfaces*, 2017, **9**, 13887–13899.
292 X. Jia, Y. Han, M. Pei, X. Zhao, K. Tian, T. Zhou and P. Liu, *Carbohydr. Polym.*, 2016, **152**, 391–397.
293 C. Sarkar, A. R. Chowdhuri, A. Kumar, D. Laha, S. Garai, J. Chakraborty and S. K. Sahu, *Carbohydr. Polym.*, 2018, **181**, 710–718.
294 M. Massaro, G. Barone, G. Biddeci, G. Cavallaro, F. Di Blasi, G. Lazzara, G. Nicotra, C. Spinella, G. Spinelli and S. Riela, *J. Colloid Interface Sci.*, 2019, **552**, 236–246.
295 M. Markman and T. M. Mekhail, *Expert Opin. Pharmacother.*, 2002, **3**, 755–766.
296 X. Wang, W. Zheng, Q. Shen, Y. Wang, Y. Tseng, Z. Luo, X. Wang, L. Shi, C. Li and J. Liu, *Signal Transduction Targeted Ther.*, 2021, **6**, 33.
297 I. J. Gomez, B. Arnaiz, M. Cacioppo, F. Arcudi and M. Prato, *J. Mater. Chem. B*, 2018, **6**, 5540–5548.
298 K. C. Nicolaou, W.-M. Dai and R. K. Guy, *Angew. Chem., Int. Ed. Engl.*, 1994, **33**, 15–44.
299 P. Ye, J. Chang, L. F. Foo and B. C. M. Yap, *Int. J. Oral Sci.*, 2017, **9**, 167–173.
300 S. M. Ardekani, A. Dehghani, P. Ye, K.-A. Nguyen and V. G. Gomes, *J. Colloid Interface Sci.*, 2019, **552**, 378–387.
301 X. He, P. Chen, J. Zhang, T.-Y. Luo, H.-J. Wang, Y.-H. Liu and X.-Q. Yu, *Biomater. Sci.*, 2019, **7**, 1940–1948.
302 K. Zhang, G. Ma, H. Wang, Z. Liang, L. Zhou and B. Yan, *J. Mater. Sci.*, 2021, **56**, 4396–4406.
303 S. Singh, A. Mishra, R. Kumari, K. K. Sinha, M. K. Singh and P. Das, *Carbon*, 2017, **114**, 169–176.
304 K. Kamimura, T. Suda, G. Zhang and D. Liu, *Pharm. Biol.*, 2011, **25**, 293–306.
305 S. O. Han, R. I. Mahato, Y. K. Sung and S. W. Kim, *Mol. Ther.*, 2000, **2**, 302–317.
306 B. Wang, J. Huang, M. Zhang, Y. Wang, H. Wang, Y. Ma, X. Zhao, X. Wang, C. Liu, H. Huang, Y. Liu, F. Lu, H. Yu, M. Shao and Z. Kang, *ACS Appl. Bio Mater.*, 2020, **3**, 8857–8864.
307 P. Chen, J. Zhang, X. He, Y.-H. Liu and X.-Q. Yu, *Biomater. Sci.*, 2020, **8**, 3730–3740.
308 Q. Wang, C. Zhang, G. Shen, H. Liu, H. Fu and D. Cui, *J. Nanobiotechnol.*, 2014, **12**, 58.
309 W. T. Godbey, K. K. Wu and A. G. Mikos, *J. Controlled Release*, 1999, **60**, 149–160.
310 L. Shen, L. Zhang, M. Chen, X. Chen and J. Wang, *Carbon*, 2013, **55**, 343–349.
311 L. Hu, Y. Sun, S. Li, X. Wang, K. Hu, L. Wang, X.-J. Liang and Y. Wu, *Carbon*, 2014, **67**, 508–513.
312 Q. Dou, X. Fang, S. Jiang, P. L. Chee, T.-C. Lee and X. J. Loh, *RSC Adv.*, 2015, **5**, 46817–46822.
313 Y. Hu, X. Geng, L. Zhang, Z. Huang, J. Ge and Z. Li, *Sci. Rep.*, 2017, **7**, 5849.
314 C. Mickaël, F. Jiahui, R. Mickaël, P. Françoise and L. Luc, *RSC Adv.*, 2019, **9**, 3493–3502.
315 K. Yang, M. Liu, Y. Wang, S. Wang, H. Miao, L. Yang and X. Yang, *Sens. Actuators, B*, 2017, **251**, 503–508.
316 T.-Y. Luo, X. He, J. Zhang, P. Chen, Y.-H. Liu, H.-J. Wang and X.-Q. Yu, *RSC Adv.*, 2018, **8**, 6053–6062.
317 W. Liu, L. Tian, J. Du, J. Wu, Y. Liu, G. Wu and X. Lu, *Analyst*, 2020, **145**(16), 5500–5507.
318 T. Vo-Dinh and B. Cullum, *Fresenius' J. Anal. Chem.*, 2000, **366**, 540–551.
319 F.-T. Wang, L.-N. Wang, J. Xu, K.-J. Huang and X. Wu, *Analyst*, 2021, **146**, 4418–4435.
320 X. Sun and Y. Lei, *TrAC, Trends Anal. Chem.*, 2017, **89**, 163–180.
321 Z. Yang, Z. Li, M. Xu, Y. Ma, J. Zhang, Y. Su, F. Gao, H. Wei and L. Zhang, *Nano-Micro Lett.*, 2013, **5**, 247–259.
322 H. Shi, J. Wei, L. Qiang, X. Chen and X. Meng, *J. Biomed. Nanotechnol.*, 2014, **10**, 2677–2699.
323 W. Ye, Y. Zhang, W. Hu, L. Wang, Y. Zhang and P. Wang, *Nanomaterials*, 2020, **10**, 2044.
324 L. Wang, H.-X. Cao, Y.-S. He, C.-G. Pan, T.-K. Sun, X.-Y. Zhang, C.-Y. Wang and G.-X. Liang, *Sens. Actuators, B*, 2019, **282**, 78–84.
325 X. Fu, L. Sheng, Y. Yu, M. Ma, Z. Cai and X. Huang, *Sens. Actuators, B*, 2018, **269**, 278–287.
326 X. Wang, D. Wang, Y. Guo, C. Yang, A. Iqbal, W. Liu, W. Qin, D. Yan and H. Guo, *Dalton Trans.*, 2015, **44**, 5547–5554.
327 X. Wu, S. Sun, Y. Wang, J. Zhu, K. Jiang, Y. Leng, Q. Shu and H. Lin, *Biosens. Bioelectron.*, 2017, **90**, 501–507.
328 I. Costas-Mora, V. Romero, I. Lavilla and C. Bendicho, *Anal. Chem.*, 2014, **86**, 4536–4543.
329 S. Ganguly, P. Das, S. Das, U. Ghorai, M. Bose, S. Ghosh, M. Mondal, A. K. Das, S. Banerjee and N. C. Das, *Colloids Surf., A*, 2019, **579**, 123604.
330 A. Barati, M. Shamsipur and H. Abdollahi, *Biosens. Bioelectron.*, 2015, **71**, 470–475.

331 J. Wang, Y. Wu, P. Zhou, W. Yang, H. Tao, S. Qiu and C. Feng, *Analyst*, 2018, **143**, 5151–5160.
332 C. Han, R. Wang, K. Wang, H. Xu, M. Sui, J. Li and K. Xu, *Biosens. Bioelectron.*, 2016, **83**, 229–236.
333 S. K. Tammina and Y. Yang, *J. Photochem. Photobiol., A*, 2020, **387**, 112134.
334 X. Yan, Y. Song, C. Zhu, H. Li, D. Du, X. Su and Y. Lin, *Anal. Chem.*, 2018, **90**, 2618–2624.
335 F. Khakbaz and M. Mahani, *Anal. Biochem.*, 2017, **523**, 32–38.
336 J. Zhang, X. Zhao, M. Xian, C. Dong and S. Shuang, *Talanta*, 2018, **183**, 39–47.
337 Z. Zhu, X. Lin, L. Wu, C. Zhao, Y. Zheng, A. Liu, L. Lin and X. Lin, *Sens. Actuators, B*, 2018, **274**, 609–615.
338 Y.-T. Yen, Y.-S. Lin, T.-Y. Chen, S.-C. Chyueh and H.-T. Chang, *R. Soc. Open Sci.*, 2019, **6**, 191017.
339 S. Liu, J. Cui, J. Huang, B. Tian, F. Jia and Z. Wang, *Spectrochim. Acta, Part A*, 2019, **206**, 65–71.
340 H. Cai, Y. Zhu, H. Xu, H. Chu, D. Zhang and J. Li, *Spectrochim. Acta, Part A*, 2021, **246**, 119033.
341 H. Wang, S. Liu, Y. Xie, J. Bi, Y. Li, Y. Song, S. Cheng, D. Li and M. Tan, *New J. Chem.*, 2018, **42**, 3729–3735.
342 H. Sies, *Redox Biol.*, 2015, **4**, 180–183.
343 L. Li, L. Shi, J. Jia, O. Eltayeb, W. Lu, Y. Tang, C. Dong and S. Shuang, *ACS Appl. Mater. Interfaces*, 2020, **12**, 18250–18257.
344 D. Wu, G. Li, X. Chen, N. Qiu, X. Shi, G. Chen, Z. Sun, J. You and Y. Wu, *Microchim. Acta*, 2017, **184**, 1923–1931.
345 M. He, N. Shang, B. Zheng and G. Yue, *RSC Adv.*, 2021, **11**, 21137–21144.
346 Q.-Y. Cai, J. Li, J. Ge, L. Zhang, Y.-L. Hu, Z.-H. Li and L.-B. Qu, *Biosens. Bioelectron.*, 2015, **72**, 31–36.
347 C. Yang, W. Deng, H. Liu, S. Ge and M. Yan, *Sens. Actuators, B*, 2015, **216**, 286–292.
348 F. Abedini, H. Hosseinkhani, M. Ismail, A. J. Domb, A. R. Omar, P. P. Chong, P.-D. Hong, D.-S. Yu and I.-Y. Farber, *Int. J. Nanomed.*, 2012, **7**, 4159–4168.
349 Y. Zhang, Y. Nie, R. Zhu, D. Han, H. Zhao and Z. Li, *Talanta*, 2019, **204**, 74–81.
350 A. H. Loo, Z. Sofer, D. Bouša, P. Ulbrich, A. Bonanni and M. Pumera, *ACS Appl. Mater. Interfaces*, 2016, **8**, 1951–1957.
351 Y. Wang, S. Wang, S. Ge, S. Wang, M. Yan, D. Zang and J. Yu, *Anal. Methods*, 2013, **5**, 1328–1336.
352 S. H. Qaddare and A. Salimi, *Biosens. Bioelectron.*, 2017, **89**, 773–780.
353 J. Kudr, L. Richtera, K. Xhaxhiu, D. Hynek, Z. Heger, O. Zitka and V. Adam, *Biosens. Bioelectron.*, 2017, **92**, 133–139.
354 S.-S. Liang, L. Qi, R.-L. Zhang, M. Jin and Z.-Q. Zhang, *Sens. Actuators, B*, 2017, **244**, 585–590.
355 N. Li, S. G. Liu, Y. D. Zhu, T. Liu, S. M. Lin, Y. Shi, H. Q. Luo and N. B. Li, *Sens. Actuators, B*, 2017, **251**, 455–461.
356 Q. Huang, Q. Li, Y. Chen, L. Tong, X. Lin, J. Zhu and Q. Tong, *Sens. Actuators, B*, 2018, **276**, 82–88.
357 Z. Wu, R. Chen, S. Pan, H. Liu and X. Hu, *Microchem. J.*, 2021, **164**, 105976.
358 X. Cheng, Y. Cen, G. Xu, F. Wei, M. Shi, X. Xu, M. Sohail and Q. Hu, *Microchim. Acta*, 2018, **185**, 144.
359 S. Xu, F. Zhang, L. Xu, X. Liu, P. Ma, Y. Sun, X. Wang and D. Song, *Sens. Actuators, B*, 2018, **273**, 1015–1021.
360 H. Zhu, E. Wang, J. Li and J. Wang, *Anal. Chim. Acta*, 2018, **1006**, 83–89.
361 M. Amjadi, T. Hallaj and Z. Kouhi, *J. Photochem. Photobiol., A*, 2018, **356**, 603–609.
362 Q. Huang, X. Lin, C. Lin, Y. Zhang, S. Hu and C. Wei, *RSC Adv.*, 2015, **5**, 54102–54108.
363 Q. Huang, S. Hu, H. Zhang, J. Chen, Y. He, F. Li, W. Weng, J. Ni, X. Bao and Y. Lin, *Analyst*, 2013, **138**, 5417–5423.
364 Q. Ye, F. Yan, D. Shi, T. Zheng, Y. Wang, X. Zhou and L. Chen, *J. Photochem. Photobiol., B*, 2016, **162**, 1–13.
365 C. Li, Y. Wang, X. Zhang, X. Guo, X. Kang, L. Du and Y. Liu, *J. Colloid Interface Sci.*, 2018, **526**, 487–496.
366 F. Yang, J. R. Wild and A. J. Russell, *Biotechnol. Prog.*, 1995, **11**, 471–474.
367 X. Gao, G. Tang and X. Su, *Biosens. Bioelectron.*, 2012, **36**, 75–80.
368 J. Hou, J. Dong, H. Zhu, X. Teng, S. Ai and M. Mang, *Biosens. Bioelectron.*, 2015, **68**, 20–26.
369 R. P. Deo, J. Wang, I. Block, A. Mulchandani, K. A. Joshi, M. Trojanowicz, F. Scholz, W. Chen and Y. Lin, *Anal. Chim. Acta*, 2005, **530**, 185–189.
370 J. Hou, Z. Tian, H. Xie, Q. Tian and S. Ai, *Sens. Actuators, B*, 2016, **232**, 477–483.
371 B. Chen, S. Chai, J. Liu, C. Liu, Y. Li, J. He, Z. Yu, T. Yang, C. Feng and C. Huang, *Anal. Bioanal. Chem.*, 2019, **411**, 2291–2300.
372 X. Wang, Y. Liu, Q. Zhou, X. Sheng, Y. Sun, B. Zhou, J. Zhao and J. Guo, *Sci. Total Environ.*, 2020, **720**, 137680.
373 D. Shi, F. Yan, T. Zheng, Y. Wang, X. Zhou and L. Chen, *RSC Adv.*, 2015, **5**, 98492–98499.
374 X. Wang, X. Li, X. Li, Y. Wang, Q. Han and J. Li, *Anal. Chim. Acta*, 2020, **1098**, 170–180.
375 K. Gao, Y. Guo, Q. Niu, L. Han, L. Zhou and L. Wang, *Sens. Actuators, B*, 2018, **262**, 298–305.
376 G. Yue, S. Li, W. Liu, F. Ding, P. Zou, X. Wang, Q. Zhao and H. Rao, *Sens. Actuators, B*, 2019, **287**, 408–415.
377 N. Xiao, S. G. Liu, S. Mo, Y. Z. Yang, L. Han, Y. J. Ju, N. B. Li and H. Q. Luo, *Sens. Actuators, B*, 2018, **273**, 1735–1743.
378 C. Wang, Z. Xu and C. Zhang, *ChemNanoMat*, 2015, **1**, 122–127.
379 M. Omidi, A. Yadegari and L. Tayebi, *RSC Adv.*, 2017, **7**, 10638–10649.
380 Y. Ma, Y. Cen, M. Sohail, G. Xu, F. Wei, M. Shi, X. Xu, Y. Song, Y. Ma and Q. Hu, *ACS Appl. Mater. Interfaces*, 2017, **9**, 33011–33019.
381 Y. Gong, B. Yu, W. Yang and X. Zhang, *Biosens. Bioelectron.*, 2016, **79**, 822–828.
382 W. Shi, F. Guo, M. Han, S. Yuan, W. Guan, H. Li, H. Huang, Y. Liu and Z. Kang, *J. Mater. Chem. B*, 2017, **5**, 3293–3299.
383 J. Zhang, H. Yang, S. Pan, H. Liu and X. Hu, *Spectrochim. Acta, Part A*, 2021, **244**, 118831.
384 N. Jing, M. Tian, Y. Wang and Y. Zhang, *J. Lumin.*, 2019, **206**, 169–175.

385 D. Y. Li, S. P. Wang, F. Azad and S. C. Su, *Ecotoxicol. Environ. Saf.*, 2020, **190**, 110141.
386 K. M. Omer and A. Q. Hassan, *Microchim. Acta*, 2017, **184**, 2063–2071.
387 L. Li, B. Yu and T. You, *Biosens. Bioelectron.*, 2015, **74**, 263–269.
388 F. Yan, Z. Bai, Y. Chen, F. Zu, X. Li, J. Xu and L. Chen, *Sens. Actuators, B*, 2018, **275**, 86–94.
389 J. Chen, Y. Li, K. Lv, W. Zhong, H. Wang, Z. Wu, P. Yi and J. Jiang, *Sens. Actuators, B*, 2016, **224**, 298–306.
390 H. N. Abdelhamid, A. Talib and H.-F. Wu, *Talanta*, 2017, **166**, 357–363.
391 H.-Y. Zhang, Y. Wang, S. Xiao, H. Wang, J.-H. Wang and L. Feng, *Biosens. Bioelectron.*, 2017, **87**, 46–52.
392 J. An, R. Chen, M. Chen, Y. Hu, Y. Lyu and Y. Liu, *Sens. Actuators, B*, 2021, **329**, 129097.
393 H. Guo, X. Wang, N. Wu, M. Xu, M. Wang, L. Zhang and W. Yang, *Anal. Methods*, 2020, **12**, 4058–4063.
394 Y. Kim and J. Kim, *Opt. Mater.*, 2020, **99**, 109514.
395 W. J. Zhang, S. G. Liu, L. Han, H. Q. Luo and N. B. Li, *Sens. Actuators, B*, 2019, **283**, 215–221.
396 M. Zhang, R. Su, J. Zhong, L. Fei, W. Cai, Q. Guan, W. Li, N. Li, Y. Chen and L. Cai, *Nano Res.*, 2019, **12**, 815–821.
397 Y. Zhang, X. Fang, H. Zhao and Z. Li, *Talanta*, 2018, **181**, 318–325.
398 A. Kumar, A. R. Chowdhuri, D. Laha, T. K. Mahto, P. Karmakar and S. K. Sahu, *Sens. Actuators, B*, 2017, **242**, 679–686.
399 Y. Jiang, Y. Wang, F. Meng, B. Wang, Y. Cheng and C. Zhu, *New J. Chem.*, 2015, **39**, 3357–3360.
400 Q. Ye, F. Yan, Y. Luo, Y. Wang, X. Zhou and L. Chen, *Spectrochim. Acta, Part A*, 2017, **173**, 854–862.
401 F. Wang, Q. Hao, Y. Zhang, Y. Xu and W. Lei, *Microchim. Acta*, 2016, **183**, 273–279.
402 L. Li, Y. Li, Y. Ye, R. Guo, A. Wang, G. Zou, H. Hou and X. Ji, *ACS Nano*, 2021, **15**, 6872–6885.
403 X. Niu, T. Song and H. Xiong, *Chin. Chem. Lett.*, 2021, **32**, 1953–1956.
404 I. Garner, R. Vichare, R. Paulson, R. Appavu, S. K. Panguluri, R. Tzekov, N. Sahiner, R. Ayyala and M. R. Biswal, *Front. Bioeng. Biotechnol.*, 2020, **8**, 1139.
405 Y. Park, Y. Kim, H. Chang, S. Won, H. Kim and W. Kwon, *J. Mater. Chem. B*, 2020, **8**, 8935–8951.
406 K. Wang, Z. Gao, G. Gao, Y. Wo, Y. Wang, G. Shen and D. Cui, *Nanoscale Res. Lett.*, 2013, **8**, 122.
407 Q. Xu, J. Gao, S. Wang, Y. Wang, D. Liu and J. Wang, *J. Mater. Chem. B*, 2021, **9**, 5765–5779.
408 N. Vale, S. Silva, D. Duarte, D. M. A. Crista, L. Pinto da Silva and J. C. G. Esteves da Silva, *RSC Med. Chem.*, 2021, **12**, 245–253.